ORIGINAL ARTICLE

MOLECULAR ECOLOGY WILEY

Genomic insights of evolutionary divergence and life history innovations in Antarctic brittle stars

Sally C. Y. Lau[1,2] | Jan M. Strugnell[1,2,3] | Chester J. Sands[4] | Catarina N. S. Silva[1] | Nerida G. Wilson[5,6,7]

[1]Centre for Sustainable Tropical Fisheries and Aquaculture and College of Science and Engineering, James Cook University, Townsville, Queensland, Australia

[2]Securing Antarctica's Environmental Future, James Cook University, Townsville, Queensland, Australia

[3]Department of Ecology, Environment and Evolution, School of Life Sciences, La Trobe University, Victoria, Melbourne, Australia

[4]British Antarctic Survey, Natural Environment Research Council, Cambridge, United Kingdom

[5]Collections & Research, Western Australian Museum, Welshpool, Western Australian, Australia

[6]School of Biological Sciences, University of Western Australia, Crawley, Western Australian, Australia

[7]Securing Antarctica's Environmental Future, Western Australian Museum, Welshpool, Western Australian, Australia

Correspondence
Sally C. Y. Lau, Centre for Sustainable Tropical Fisheries and Aquaculture and College of Science and Engineering, James Cook University, Townsville, Queensland, Australia.
Email: cheukying.lau@jcu.edu.au

Abstract

Understanding the drivers of evolutionary innovation provides a crucial perspective of how evolutionary processes unfold across taxa and ecological systems. It has been hypothesised that the Southern Ocean provided ecological opportunities for novelty in the past. However, the drivers of innovation are challenging to pinpoint as the evolutionary genetics of Southern Ocean fauna are influenced by Quaternary glacial–interglacial cycles, oceanic currents and species ecology. Here we examined the genome-wide single nucleotide polymorphisms of the Southern Ocean brittle stars *Ophionotus victoriae* (five arms, broadcaster) and *O. hexactis* (six arms, brooder). We found that *O. victoriae* and *O. hexactis* are closely-related species with interspecific gene flow. During the late Pleistocene, *O. victoriae* likely persisted in a connected deep water refugium and in situ refugia on the Antarctic continental shelf and around Antarctic islands; *O. hexactis* persisted exclusively within in situ island refugia. Within *O. victoriae*, contemporary gene flow linking to the Antarctic Circumpolar Current, regional gyres and other local oceanographic regimes was observed. Gene flow connecting West and East Antarctic islands near the Polar Front was also detected in *O. hexactis*. A strong association was detected between outlier loci and salinity in *O. hexactis*. Both *O. victoriae* and *O. hexactis* are associated with genome-wide increase in alleles at intermediate-frequencies; the alleles associated with this peak appear to be species specific, and these intermediate-frequency variants are far more excessive in *O. hexactis*. We hypothesise that the peak in alleles at intermediate frequencies could be related to adaptation in the recent past, linked to evolutionary innovations of increase in arm number and a switch to brooding from broadcasting, in *O. hexactis*.

KEYWORDS
echinoderms, life history evolution, molecular evolution, population genetics-empirical

[Correction added on 12 May 2023, after first online publication: article title has been corrected to replace "histories" with "history".]

1 | INTRODUCTION

Evolutionary innovation fuels the complexity among species differences and the overall diversity in the global ecosystem (Arnold & Kunte, 2017; McGee et al., 2015). Innovations can be defined as the impacts of novelties (Erwin, 2021). While the definition of novelty can be broad, it is commonly defined as trait expression or novel function across a broad range of behavioural, physiological and morphological characteristics (Love, 2003; Moczek et al., 2011). Although innovations can be found everywhere in the natural world, the drivers of these are often unclear, as processes differ among taxa and ecological systems (Wagner, 2011). Understanding evolutionary changes between closely-related species offers valuable opportunities to pinpoint past demographic events and genotypic signatures linked to novelties, which in turn can reveal the unique environmental and biological 'building blocks' of innovative evolutionary processes.

Evolutionary innovation among specific closely-related species has been discussed within environmental and/or ecological contexts in the marine realm outside the Southern Ocean. In echinoderms, contrasting reproductive strategies (brooding vs broadcasting) have been observed in closely-related brittle stars in the genus *Ophioderma* from the Mediterranean (Boissin et al., 2011). Divergent life histories (planktotrophy vs lecithotrophy) have also been examined within *Heliocidaris* sea urchins (Davidson et al., 2022). There is also evidence that the Southern Ocean could have provided ecological opportunities for evolutionary innovation in the past, with cases linked to the onset of polar conditions ~33 Ma (Daane et al., 2019) and the recent Quaternary glacial–interglacial cycles (~2.58 Ma–now) (Lau et al., 2021; Wilson et al., 2013). The Southern Ocean contains a high diversity of marine benthic fauna (~88% of total Antarctic marine species, De Broyer et al., 2011), with most modern taxa have diversified and persisted in situ since the Mid-Miocene (c. 14 Mya, Crame, 2018). The apparent ecological success of the Southern Ocean benthic fauna has been structured by Quaternary glacial–interglacial cycles when the Antarctic ice sheet (AIS) repeatedly expanded and contracted over time. At extreme glacial cycles in the late Pleistocene, the AIS expanded with grounded ice (i.e. resting on the seafloor) reaching the edge of the Antarctic continental shelf (Anderson et al., 2002), which eroded most of the continental shelf seafloor habitat. Throughout extreme glacial maxima, Southern Ocean benthic fauna could have remained within in situ small-scale ice-free refugia on the shelf, migrated to the deep sea or to Antarctic islands off the shelf (Brey et al., 1996; Convey et al., 2009; Crame, 1997; Kott, 1969; Thatje et al., 2005). Nonetheless, evidence regarding where and how benthic taxa survived the Pleistocene glacial period remains limited (Lau et al., 2020). Over time, species diversification and gene flow have also been influenced by regional oceanography (Muñoz-Ramírez et al., 2020) and the broader Antarctic Circumpolar Current (ACC, González-Wevar et al., 2017; Moore et al., 2018). More importantly, how these different events and processes (e.g. glacial survival + oceanic currents + species dispersal and adaptation) structured genetic patterns

simultaneously over time and across spatial scales are unclear (Lau & Strugnell, 2022).

Only species with a circum-Antarctic distribution can offer comprehensive phylogeographic patterns to answer broad evolutionary questions specific to the Southern Ocean. These questions have rarely been investigated thoroughly due to limited sample availability from the region, and a lack of prior knowledge of species ecology and evolutionary history. Many key Southern Ocean regions, particularly East Antarctica (two-thirds of the Antarctic continent), Antarctic islands and the deep sea, are scarcely sampled as they are located away from national research stations (Griffiths et al., 2014). Compounding this issue, biological samples are often stored at room temperature in long-term museum collections (De Broyer et al., 2011), leading to DNA degradation. Investigation of innovation also requires comprehensive surveys of closely-related species. This presents additional challenges as it requires knowledge of species' taxonomy, phylogeny and life history, examined for a few Southern Ocean benthic taxa (Riesgo et al., 2015; Xavier et al., 2016).

The Southern Ocean brittle stars *Ophionotus victoriae* and *O. hexactis* are excellent candidates to test for explanatory evolutionary processes across the Southern Ocean. The brittle star *Ophionotus victoriae* Bell, 1902 is commonly found on the Antarctic continental shelf and around Antarctic islands south of the Polar Front (PF) (Sands et al., 2013). It has a circumpolar distribution and has been collected from shallow depths to deep sea (Lau et al., 2021). Furthermore, a close phylogenetic relationship between *O. victoriae* and *O. hexactis* E. A. Smith, 1876, has been proposed by multiple genetic studies (cytochrome c oxidase subunit I (COI) and exon genomic data, Galaska et al., 2017; Hugall et al., 2016), with incomplete lineage sorting suggested between them (Lau et al., 2021). *Ophionotus hexactis* is commonly found around Antarctic islands near the PF and is mainly distributed at shallow depths (0–302 m) (McClintock, 1994; this study). The genetic closeness between *O. victoriae* and *O. hexactis* is striking, as the two species have different morphological and functional traits; *O. victoriae* is characterized by five arms and pelagic planktotrophic larvae (Grange et al., 2004), and *O. hexactis* by six arms and brooding juveniles (Turner & Dearborn, 1979). Given that the phylotypic characters of extant echinoderms (including brittle stars) are pentameral symmetry (Arnone et al., 2015) and pelagic planktotrophic larvae (Gillespie & McClintock, 2007), it has been hypothesized that the divergent characteristics of *O. hexactis* could be innovations linked to survival within glacial refugia around Antarctic islands throughout the Pleistocene (Lau et al., 2021).

Here, we investigate the evolutionary histories of *O. victoriae* and *O. hexactis* with double-digest restriction-associated DNA (ddRAD) loci, using samples collected throughout most of their distributional range between scuba diving depths and 1750 m. We utilized a target capture approach to sequence ddRAD-identified loci in degraded samples from museum collections, which enabled comprehensive sampling. Specifically, we examined the genealogical relationship between *O. victoriae* and *O. hexactis*, signatures of Pleistocene glacial refugia (deep-sea refugia, in situ continental shelf and Antarctic

island refugia) in *O. victoriae* and *O. hexactis*, and the evolutionary context behind innovations in *O. hexactis*.

2 | METHODS

2.1 | Samples and sequencing

Target capture of ddRAD loci data was sequenced from degraded tissue samples of *O. victoriae* ($n = 218$) and *O. hexactis* ($n = 40$, Table S1-S9). Informative loci were first identified from ddRAD sequencing between eight mitochondrially divergent *Ophionotus* individuals (including both species) that possessed high-quality gDNA (Appendix S1: Supplementary Information Note 1). All target capture libraries were enriched in capture reactions using Arbor myBaits® following the manufacturer's protocol and resulting capture reactions were sequenced on Illumina NovaSeq S4 with 150 basepair (bp) paired-end reads. See Appendix S1: Supplementary Information Note 1 for further sequencing information.

2.2 | Target capture data processing, reads mapping and variant calling

Raw data were demultiplexed with barcodes removed using *process_shortreads* in *Stacks* v2.3d (Catchen et al., 2013). Reads with phred quality less than 20 (Q < 20) and polyG in read tails discarded using *fastp* v0.20 (Chen et al., 2018). Potential contaminants (human and microorganisms) were identified using *Kraken* v1.0 (Wood & Salzberg, 2014), and reads that matched those of the contaminant database were removed. Reads were then truncated to a final read length of 140 bp. Cleaned and trimmed reads were checked for quality using *fastQC* v0.11.7 (Andrews, 2010) and mapped to the consensus sequences of ddRAD loci used for bait design using *bwa* v0.7.17 *mem* with default parameters (Li & Durbin, 2009). *Samtools* v1.7 (Li et al., 2009) was used to sort alignments by coordinates, and PCR duplicates were removed using *picard* v2.18.1 (Broad Institute, 2019). Variants and short indels were called across all samples using *bcftools* v1.7 *mpileup* (Li et al., 2009) for variant filtering.

2.3 | Variant filtering

Three SNPs data sets were created for subsequent analyses, and *VCFtools* was used to perform variant filtering on the raw variant calls. Prior to SNP filtering, the first data set included both *O. victoriae* and *O. hexactis*, the second data set included only *O. victoriae* and the third data set included only *O. hexactis*. Within all three data sets, indels and samples with high missing data on an individual basis (>80%) were first removed, and high-quality SNPs were retained as follows. First, sites with Phred scaled site quality score more than 30 were kept (−minQ 30). Then, sites with mean read depth of less than 10x and greater than 32x (=2*average

depth (15.8x)) were removed (−min-meanDP 10, −max-meanDP 32). Sites were kept if they were biallelic (−min-alleles 2, −max-alleles 2), and if present in 70% of all samples (−max-missing 0.7), and with a minor allele frequency of at least 2% were kept (−maf 0.02). To remove sites that likely belonged to paralogous loci and therefore artificial SNPs, only sites with a maximum observed heterozygosity of 0.5 were kept (Gargiulo et al., 2020; Hohenlohe et al., 2011) (identified via the R package *adegenet* v2.1.3, Jombart & Ahmed, 2011). Lastly, only one site per locus was kept (−thin 140). The final data sets included *O. victoriae* ($n = 155$) and *O. hexactis* ($n = 40$) with 1781 SNPs in data set 1, *O. victoriae* ($n = 158$) with 1653 SNPs in data set 2 and *O. hexactis* ($n = 40$) with 2209 SNPs in data set 3.

2.4 | Genetic structure within and between species

The overall levels of genetic differentiation between species, and among sample locations within species, were assessed via population statistics. The inbreeding coefficient (F_{IS}) was calculated using *GenoDive* v3.0 (Meirmans, 2020). Neutrality tests, including Tajima's D and Fu's F_S tests, were calculated using the R package *PopGenome* v2.7.5 (Pfeifer et al., 2014). To gain a broader perspective of the relationship between species, Tajima's D and Fu's F_S between species were also calculated excluding samples that exhibited strong signatures of intraspecific admixture, that is *O. victoriae* from South Georgia ($n = 2$) and *O. hexactis* from Bransfield Mouth ($n = 10$, Figure 1).

Principal Component Analyses (PCA) and Discriminant Analysis of Principal Components (DAPC) were performed using *adegenet* to examine the species boundaries between *O. victoriae* and *O. hexactis* (data set 1), whether genetically distinct clusters were present within *O. victoriae* and *O. hexactis* (data sets 2 and 3), as well as how genetic variation might be related to signatures of Pleistocene glacial refugia in *O. victoriae* (data set 2). PCA assumes overall variability among samples that includes between- and within-group variations, whereas DAPC assumes genetic differentiation between groups while overlooking within-group variation (Balaško et al., 2022). As the Antarctic continental shelf extends down to ~1000 m due to the weight of previous ice sheets, following Clarke and Johnston (2003), we defined glacial refugia categories as follow: continental shelf localities > 1000 m and < 1000 m to be related to deep-water refugia and in situ continental shelf refugia, respectively; and Antarctic island localities to be related to in situ island refugia. See Appendix S1: Figure S1 for a map of the Southern Ocean with sample distribution and bathymetry outlined.

For *O. victoriae*, a hierarchical analysis of molecular variance (AMOVA) was also used to estimate variation at three hierarchical subdivisions (among putative refugia types 'deep water refugia/ in situ continental shelf refugia/in situ Antarctic island refugia', among geographical locations within each putative refugia type, and within the sampled locations). AMOVA was performed using *poppr* (Kamvar et al., 2014) with 999 permutations to evaluate
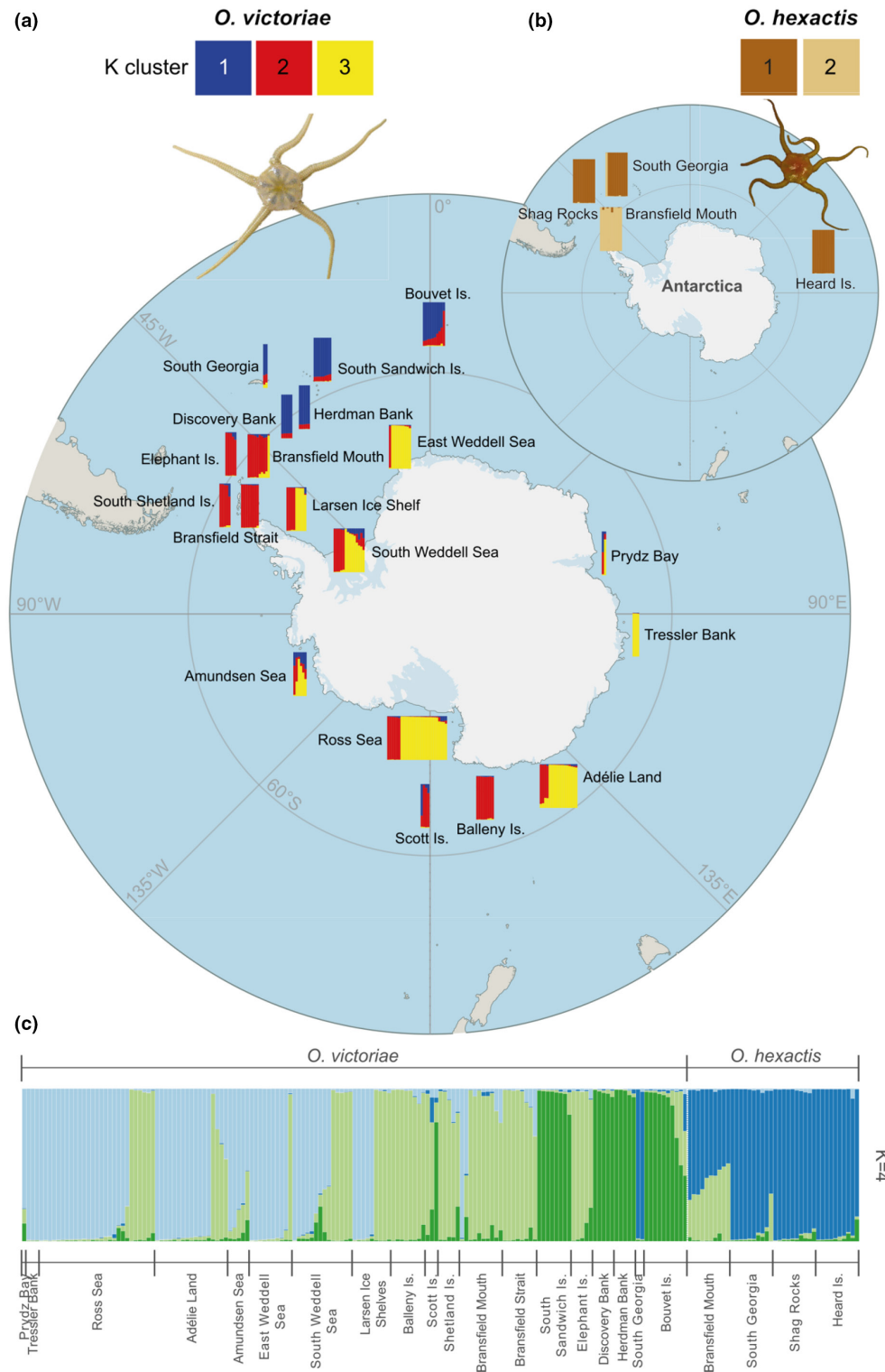
FIGURE 1 Map of Southern Ocean with sampling locations and admixture proportions within *Ophionotus victoriae* with pelagic larvae (a) ($n = 158$) and *O. hexactis* with brooded juveniles (b) ($n = 40$). (c) Admixture proportions between *O. victoriae* and *O. hexactis* ($n = 195$). Each vertical bar represents one individual sample, colours correspond to admixture proportion estimations derived from *Structure* analyses (only optimal values of *K* are presented in the main figure).

significance levels. The alleles contributing the most to the discriminant functions (at 0.999 quantile) between *O. victoriae* and *O. hexactis* (data set 1) were also examined using a DAPC loading plot via *adegenet*.

Genetic structure between species (using data set 1), and among sample locations within species (using data sets 2 and 3) were also examined via *Structure* v2.3.4 (Pritchard et al., 2000). *Structure* was performed to assign individuals to genetic clusters

(K). *Structure* was run for K = 1–10 with 10 replicates per K via *Structure_threader* (Pina-Martins et al., 2017). Each run was performed with 500,000 iterations and a burn-in of 100,000. Prior information of species information (data set 1) or sample location (data sets 2 and 3) was utilized via LOCPRIOR 1 to assist clustering without artificially inflating genetic structure (see Pritchard et al., 2000). The meaningful K per data set was evaluated based on the highest mean log-likelihood [mean LnP(K)] and deltaK statistics using *Structure Harvester* v0.6.94 (Earl & Von Holdt, 2012). Each population structure inference has its limitations, eg., *Structure* may not produce reliable structure estimates when the uneven sample size is involved (Puechmaille, 2016), and it could over- or underestimate population genetic structure (Janes et al., 2017). Therefore, we interpret population structure based on evaluating the findings in the context of multiple analyses (PCA, DAPC and *Structure*).

2.5 | Population tree with admixture

TreeMix v1.13 (Pickrell & Pritchard, 2012) was performed to infer a maximum likelihood (ML) tree topology within each species, as well as to calculate a covariance matrix to infer historical splits and mixture between populations, using data set 1 (1781 SNPs). For *TreeMix* analysis within *O. victoriae*, all individuals of *O. hexactis* were assigned as an outgroup for tree rooting. From Thom et al. (2020), populations within *O. victoriae* were manually classified by clustering individuals from neighbouring sample locations with similar admixture proportions based on the *Structure* analysis (optimal K = 4 in data set 1). For *TreeMix* analysis within *O. hexactis*, all individuals of *O. victoriae* were assigned as an outgroup. Populations within *O. hexactis* were manually classified by sample sites, as the genetic structure of *O. hexactis* can be defined by geographical locations (based on *Structure* analysis of data set 1).

Migration edges (m) were modelled between 0 and 10 in *O. victoriae* and between 0 and 5 in *O. hexactis*; fewer m was explored in *O. hexactis* since only four localities were sampled for this species. Ten replicates per each migrant edge were generated following Fitak (2021), and the bootstrap option with a block size of 1 enabled. The best *TreeMix* model with the optimal number of migration edges for each species was evaluated based on residuals of the covariance matrix as well as the simple exponential and nonlinear least square model (threshold = 0.05) using the R package *OptM* v0.1.3 (Fitak, 2021). Confidence of migration events was evaluated using jackknife p values, f_3 and f_4 statistics implemented within *TreeMix*.

2.6 | Gene flow within and between species

Genetic differentiation between species (data set 1) and among locations within species (data set 2 and 3) was examined with pairwise F_{ST} values, which were calculated using *GenoDive* with 10,000 permutations to test for significance. Post hoc Bonferroni correction was applied to account for multiple pairwise comparisons. When calculating pairwise F_{ST} between locations within *O. victoriae*, samples from South Georgia were excluded due to low sample size (n = 2). Samples of *O. victoriae* from Tressler Bank (n = 3) and Prydz Bay (n = 2) were also pooled together and defined as 'East Antarctica' in order to increase overall sample size and to evaluate the genetic differentiation between East Antarctica versus West Antarctic and Antarctic island localities.

2.7 | Genotype environmental association analysis

Redundancy analyses (RDA) were performed to detect genome-wide adaptations to environmental variables in the Southern Ocean, specifically the proportion of genetic variation explained by each identified environmental predictor within a multivariate environment, as well as the putative outlier SNPs with significant statistical associations with environmental predictors. Environmental data from each sample location (sea surface temperature and salinity, water bottom temperature and salinity) were extracted from World Ocean Atlas 2018 (Locarnini et al., 2018; Zweng et al., 2018), using *QGIS* (QGIS Development Team, 2019), following Lau et al. (2021).

RDA were performed using the R package *vegan* v2.5–6 (Oksanen et al., 2013), and separate RDA were performed (a) between samples of *O. victoriae* and *O. hexactis* (data set 1), (b) among samples within *O. victoriae* with samples separated by deep continental shelf (>1000m), shallow continental shelf (<1000m) and Antarctic islands (data set 2) and (c) among sample locations within *O. hexactis* (data set 3). Within each RDA, multicollinearity between environmental predictors was assessed using the R package *psych* v1.9.12 (Revelle, 2020, cut-off threshold at r = 0.7). In the RDA between *O. victoriae* and *O. hexactis* and within *O. victoriae*, variables of sea surface temperature and salinity, water bottom temperature and salinity, water depths and longitudes were retained. For *O. hexactis*, only the variables of water bottom temperature and salinity, and water depths were retained.

The significance (at α = 0.05) of each full RDA model was assessed via ANOVA with 999 permutations, and Variance Inflation Factors were assessed for further evidence of multicollinearity between environmental predictors within each RDA model. RDA was also used to identify the SNP loadings in the ordination space to assess whether SNPs are associated with environmental predictors (i.e. SNPs under selection as a function of environmental predictors). Outlier SNPs were identified through the distribution of SNP loadings on each significant RDA axis. SNPs that exhibit more than ±3 standard deviation from the mean loading were identified as outliers, a threshold that minimizes type I and II error (Forester et al., 2018). Associations between putative outlier SNPs and environmental variables were evaluated using the Pearson correlation coefficient.

2.8 | Outlier loci detection and gene ontology

Loci under putative selection within and between species were identified using genetic differentiation outlier analyses; *OutFLANK* v.02 (Whitlock & Lotterhos, 2015), *BayeScan* v2.1 (Foll & Gaggiotti, 2008), *PCAdapt* v4.3.2 (Privé et al., 2020) and RDA. For *OutFLANK* and *BayeScan*, individuals can be pre-defined in different populations and thus samples were grouped between species (data set 1) and within species (data sets 2 and 3). Between species (data set 1), samples for *O. victoriae* from South Georgia ($n = 2$) were categorized as *O. hexactis* due to their limited genetic differentiation from *O. hexactis*. Within *O. victoriae* (data set 2), samples were separated among those collected from the deep continental shelf (>1000 m), shallow continental shelf (<1000 m) and around Antarctic islands (glacial refugia categories). Within the *O. hexactis* (data set 3), samples were separated among sample locations.

For *BayeScan* analyses, prior odds were set to 100, followed by 20 pilot runs and 100,000 iterations with 5000 samples, a burn-in length of 50,000 and a thinning interval of 10. *OutFLANK* analyses were performed using default parameters and a *q*-value threshold of 0.01. *PCAdapt* analyses were performed with scree plots used to select the optimal principal component (K), and outlier SNPs were determined via the Benjamini-Hochberg Procedure with a p-value threshold (alpha) of 0.01.

Loci that were identified as outliers by two or more tests (*OutFLANK*, *BayeScan*, *PCAdapt*, RDA) were considered to be putatively under selection. The consensus sequences (140 bp) of all putative outlier loci were compared within the National Center for Biotechnology Information (NCBI) database (Agarwala et al., 2018) using the BLASTx (Altschul et al., 1990) search tool to determine their identities. Hits returned with a maximum E value of 1×10^{-3} and a per cent identity of at least 80% were considered significant matches. The consensus sequences of outlier loci were also translated to protein sequences in all six reading frames (standard code) and were searched against the *InterPro* (Blum et al., 2021) protein database using *InterProScan* (Jones et al., 2014) in *Geneious* (https://www.geneious.com). *InterProScan* results were also used to infer gene ontology IDs.

2.9 | *ANGSD* filtering for SFS-based inferences

For past demographic inference (*dadi* v2.1.1, Gutenkunst et al., 2009) and *StairwayPlot* v2.1.1 (Liu & Fu, 2015, 2020) analyses, we generated site frequency spectrum (SFS) using genotype-likelihood estimations via *ANGSD*. For SFS-based inferences, genotype-likelihood estimation was used instead of genotype calling as our data are characterized by low-medium coverage. Genotype-likelihood estimation approach enables us to retain low-frequency variants that are highly valuable for SFS-based inferences, while accounting for potential errors associated with low coverage (Korneliussen et al., 2014). Following Lesturgie et al. (2021), we first generated site frequency likelihood files with genotype likelihoods computed with the samtools method (−GL =1). We applied the following filters: (1) removed sites with coverage <3 (−minIndDepth =3), (2) removed poor quality

bases and poorly aligning reads (−minQ 20 and −minMapQ 30 and −C 50), (3) removed poor quality sites based on the per-base alignment quality (−baq =1), (4) removed SNPs in the last 5 bp of each locus, (5) SNPs heterozygous in at least 80% of individuals and (6) sites must be present in at least 80% of individuals. We first used *RealSFS* to generate unfolded SFS and then used *dadi* to fold and down-project SFS for downstream analyses. Separate estimations of genotype-likelihood were applied to different data sets depending on the analytical approaches (see below).

For all SFS-based inferences, a generation time of 9 years was assumed based on information about minimum disc size at sexual maturity (based on females) (Grange et al., 2004) and average disc size across the age of *O. victoriae* (Dahm & Brey, 1998). A mutation rate of 1.43×10^{-8} per site per generation was used based on the tip substitution rate of the *O. victoriae* and *O. hexactis* branch among global ophiuroid species (0.0015924; substitution/site/myr) (O'Hara et al., 2019). It should be noted that estimates of mutation rates from phylogenies are likely not representative of germline mutation rates in shorter times due to heterotachy (Phillips, 2009). However, currently, there is no genome-wide mutation rate estimated for echinoderms to our knowledge, the mutation rate calculated from phylogenies is the only meaningful rate that can be incorporated at present.

2.10 | Past population size changes within species

Past effective population size (N_e) changes within *O. victoriae* and *O. hexactis* were reconstructed using *StairwayPlot*. *StairwayPlot* is a model-flexible method that infers past population size changes over specific points in genealogy through one-dimensional site frequency spectrum (1d SFS). *Stairway plot* was chosen to further explore past population size changes within species instead of demographic models (e.g. *dadi*) as it is not constrained by a priori information, which can in turn explore a larger model space than parametrised demographic models (Liu & Fu, 2015). For StairwayPlot, down projection was performed in order to maximize the number of segregating sites. Within *O. victoriae*, we explored 1d SFS in samples collected from deep water (>1000 m), continental shelf (<1000 m) and around Antarctic islands. Down projection was achieved at 18, 92 and 80 haploid samples, respectively. Within *O. hexactis*, we explored 1d SFS in samples from Bransfield Mouth and other localities (Shag Rocks, South Georgia, Heard Island pooled together). Down projection was achieved at 14 and 40 haploid samples, respectively.

Each run was performed with a random starting seed. The percentage of sites used for training was 67% and the number of random breakpoints for each run were (nseq-2)/4, (nseq-2)/2, (nseq-2)*3/4, nseq-2 based on default values.

2.11 | Demographic modelling between *O. victoriae* and *O. hexactis*

The divergence and connectivity between *O. victoriae* and *O. hexactis* were investigated via the diffusion approximation framework

within *dadi*. We explored the relationship between *O. victoriae* and *O. hexactis* using all samples from both species, but excluded samples with signals of strong interspecific admixture, that is *O. victoriae* from South Georgia ($n=2$) and *O. hexactis* from Bransfield Mouth ($n=10$), thus the total sample size was n=183. A total of nine demographic models (Appendix S1: Supplementary Note 2) were fitted against the folded two-dimensional joint site frequency spectrum (2d jSFS) between *O. victoriae* and *O. hexactis*. The examined demographic models ranged from simple (three parameters) to complex (10 parameters) biologically-relevant scenarios, including divergence followed by strict isolation, continuous migration, ancient migration, secondary contact and past population size changes (Appendix S1: Figure S2).

Input dataset was 50% down projected to (haploid $n=153$ in *O. victoriae*, $n=30$ in *O. hexactis*) in order to maximize the number of segregating sites for *dadi*, as recommended by Gutenkunst et al. (2009). Each *dadi* model was run with four consecutive rounds of optimization using the *dadi_pipeline* v3.1.6 with default features (Portik et al., 2017). Parameters of the best-fit model were converted into biologically meaningful units. For a detailed description of *dadi* inference and model evaluations, see Appendix S1: Supplementary Information Note 2.

3 | RESULTS

3.1 | Read quality

A total of 83,789,628 raw reads were obtained from the eight *Ophionotus* samples during ddRAD loci discovery, with an average of 10,473,704 reads $\pm2,042,156$ SD per sample. After SNP filtering for no missing data and maf of at least 1%, the loci discovery dataset included 8113 ddRAD loci for target capture bait design (see Appendix S1: Supplementary Note 1). After target capture sequencing of all *Ophionotus* samples ($n=258$), a total of 847,967,674 raw reads were obtained, with an average of 4,583,609 reads $\pm2,543,496$ SD per sample, as well as an average depth of 15.8x (across sites per sample).

3.2 | Genetic diversity and population structure

Overall, both *O. victoriae* and *O. hexactis* exhibited negative inbreeding coefficients (Table 1). Both species and all their respective sample localities were associated with negative Tajima's D values (Table 1). Negative Fu's Fs values were also observed across *O. victoriae* (all sequences pooled together) as well as in *O. victoriae* from Ross Sea, Adélie Land, east Weddell Sea, south Weddell Sea, Bransfield Mouth and Bouvet Island (Table 1). Positive Fu's Fs values were observed across *O. hexactis* and within collected localities.

PCA indicated an overall separation between *O. victoriae* and *O. hexactis*, with 4.35% of the total genetic variance explained by the first two PCs (Figure 2a). DAPC results are also in agreement

with PCA, which demonstrated two broad genetic clusters observed between species (Appendix S1: Figures S3, S4). From PCA, two *O. victoriae* samples (ID: SIOBICE6508 and SIOBICE6420) from South Georgia were observed within the *O. hexactis* cluster (Figure 2a). On PC1 and PC2 axes, individuals of *O. victoriae* from Scott Island, Bouvet Island and Bransfield Mouth also showed close proximity to *O. hexactis* from Bransfield Mouth (Appendix S1: Figure S5).

Genotypic clustering using *Structure* suggested that $K=2$ and $K=4$ are useful indications of admixture proportions across *O. victoriae* and *O. hexactis* samples (Figure 1, Appendix S1: Figure S6), and the PCA and DAPC results also supported the $K=4$ model. *Structure* also suggested that at $K=4$, *O. hexactis* was represented overall by a distinct genetic cluster, but *O. victoriae* from South Georgia cannot be differentiated from *O. hexactis* (Figure 1). Individuals of *O. hexactis* from Bransfield Mouth were distinct from *O. hexactis* from other locations by displaying genetic admixture with *O. victoriae* (most notably from Bransfield Mouth, Bransfield Strait, Elephant Island, South Shetland Islands and Balleny Islands). Three loci (CLocus-61907, CLocus-137845 and CLocus-172167) were identified as the most contributing variables to the discriminant functions at 0.999 quantiles (Appendix S1: Figure S7). Major and minor allele frequency at these three loci were also examined between species, with *O. victoriae* from South Georgia and *O. hexactis* from Bransfield Mouth also visualized as separate clusters. At CLocus-61907, *O. victoriae* from South Georgia shares similar allele frequencies with *O. hexactis* samples. At CLocus-137845 and CLocus-172167, major and minor allele frequencies were similar between *O. victoriae* (overall) and *O. hexactis* from Bransfield Mouth as well as *O. hexactis* (overall) and *O. victoriae* from South Georgia (Appendix S1: Figure S7).

Within *O. victoriae*, when samples are grouped by geographical locations, PCA indicated an overall limited genetic variation across localities, while South Sandwich Islands, Discovery Bank and Herdman Bank are slightly separated from the rest of sampled localities (Appendix S1: Figure S5b). Pairwise F_{ST} analysis supported no significant differentiation was observed between most areas (Table S1-S9). *Structure* suggested that at $K=3$, *O. victoriae* individuals from the continental shelf and Antarctic islands were generally separated by distinct genetic clusters (Figure 1). This is congruent with DAPC, where three clusters were observed along the PC1 axis and mostly correspond to the distributions of the three K clusters detected within *Structure* (Appendix S1: Figure S9-S10). When samples were grouped based on glacial refugia categories, PCA showed clear divergence within shallow continental shelf (i.e. the signature of persistence within in situ continental shelf refugia) and Antarctic islands (i.e. the signature of persistence within island refugia), while also exhibiting connectivity between these two habitats which is expected for species with pelagic larvae (Figure 2b). Samples from the deep continental shelf (>1000m) are uniquely similar on both PC axes, despite being collected around the vast Antarctic continent (Figure 2b), indicating a preliminary signature of connectivity within in situ deep-water refuge. *Structure* further indicated samples from the deep continental shelf (>1000m) exhibit a higher level of admixture

TABLE 1 Genetic diversity and neutrality test results of *Ophionotus victoriae* and *O. hexactis* across geographical locations based on target capture sequencing of ddRAD loci.

	Sampled depth range (m)	Number of samples	Inbreeding coefficient (F_{IS})	Tajima's D	Fu's Fs
O. victoriae					
Continental shelf					
All	0–1750	158	−0.157	−1.272	−1.459
Prydz Bay	213–270	2	−0.109	NA	2.866
Tressler Bank	758–779	3	−0.140	−1.106	2.718
Ross Sea	0–1376	27	−0.141	−1.169	−5.905
Adélie Land	22–1204	17	−0.138	−1.284	−2.335
Amundsen Sea	998–1208	6	−0.196	−0.150	1.269
East Weddell Sea	250–615	10	−0.152	−1.077	−0.143
South Weddell Sea	282–1750	14	−0.133	−1.272	−1.459
Larsen Ice Shelf	320–682	9	−0.133	−1.276	0.076
Antarctic islands					
Balleny Islands	85–350	8	−0.146	−1.113	0.425
Scott Island	144–403	4	−0.194	NA	1.904
South Shetland Islands	183	5	−0.148	−0.940	1.524
Bransfield Mouth	302–349	10	−0.150	−0.893	−0.164
Bransfield Strait	213–292	8	−0.142	−1.162	0.375
South Sandwich Islands	116–230	8	−0.164	−1.047	0.340
Elephant Island	143–202	5	−0.134	−1.183	1.500
Discovery Bank	439	5	−0.185	−0.876	1.510
Herdman Bank	600	5	−0.182	−0.512	1.502
South Georgia	167–190	2	−0.195	NA	3.489
Bouvet Island	300	10	−0.164	−0.872	−0.319
O. hexactis					
Antarctic islands					
All	131–302	40	−0.144	−1.188	0.260
Bransfield Mouth	302	10	−0.168	−0.969	0.257
South Georgia	119	10	−0.132	−1.244	0.286
Shag Rocks	131–180	10	−0.138	−1.169	0.313
Heard Island	203	10	−0.137	−1.188	0.260

with Antarctic islands, bypassing the shallow continental shelf (<1000 m, Appendix S1: Figure S8). Focusing on *O. victoriae* samples, AMOVA results further indicated significant molecular variances derived from all tested hierarchical subdivisions (among putative refugia types [1.91%, *p* < .001]), among geographical locations within each putative refugia type [2.71%, *p* < .001], and within geographical locations [95.38%, *p* < .001] (Table S1-S9).

Within *O. hexactis*, PCA indicated an overall difference between samples from Bransfield Mouth and other locations (South Georgia, Shag Rocks and Heard Island) (Figure 2c). One sample from South Georgia was found within the Bransfield Mouth cluster. A lack of genetic differentiation was observed between samples from South Georgia and Shag Rocks. Samples from South Georgia and Shag Rocks also showed limited differentiation from those from Heard Island. Pairwise F_{ST} values suggested significant difference between individual sample localities (*p* < .001; Table S1-S9).

Structure suggested that at *K* = 2, samples from Bransfield Mouth (+ one sample from South Georgia) were characterized by a distinct genetic cluster, with no differentiation observed between samples from South Georgia, Shag Rocks and Heard Island (Figure 1). DAPC also indicated congruent results to PCA, Pairwise F_{ST} and Structure; DAPC recovered 5 genetic clusters in *O. hexactis*, with samples from the mouth of the Bransfield Straight being distinctly different from other locations, and samples from other locations exhibiting clear gene flow between them (Appendix S1: Figure S11-S12).

3.3 | Population tree with admixture within species

Within *O. victoriae*, *TreeMix* (explained 90.2% of the total variance) revealed samples from South Georgia were closely related to *O.*
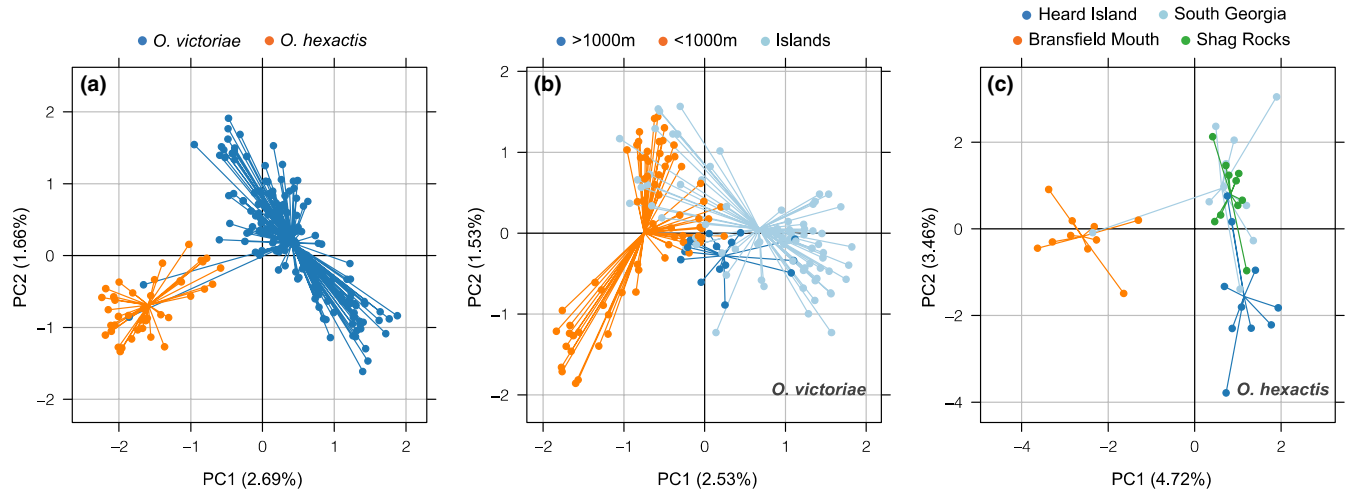
FIGURE 2 Principal component analysis (PCA) results on the first two axes including (a) samples of *Ophionotus victoriae* and *O. hexactis*; (b) within *O. victoriae* with samples grouped by glacial refugia categories, those collected on the deep Antarctic continental shelf (>1000 m), shallow Antarctic continental shelf (<1000 m) and around Antarctic islands (off the Antarctic continental shelf, south of Polar Front); (c) within *O. hexactis* with samples grouped by geographical locations.
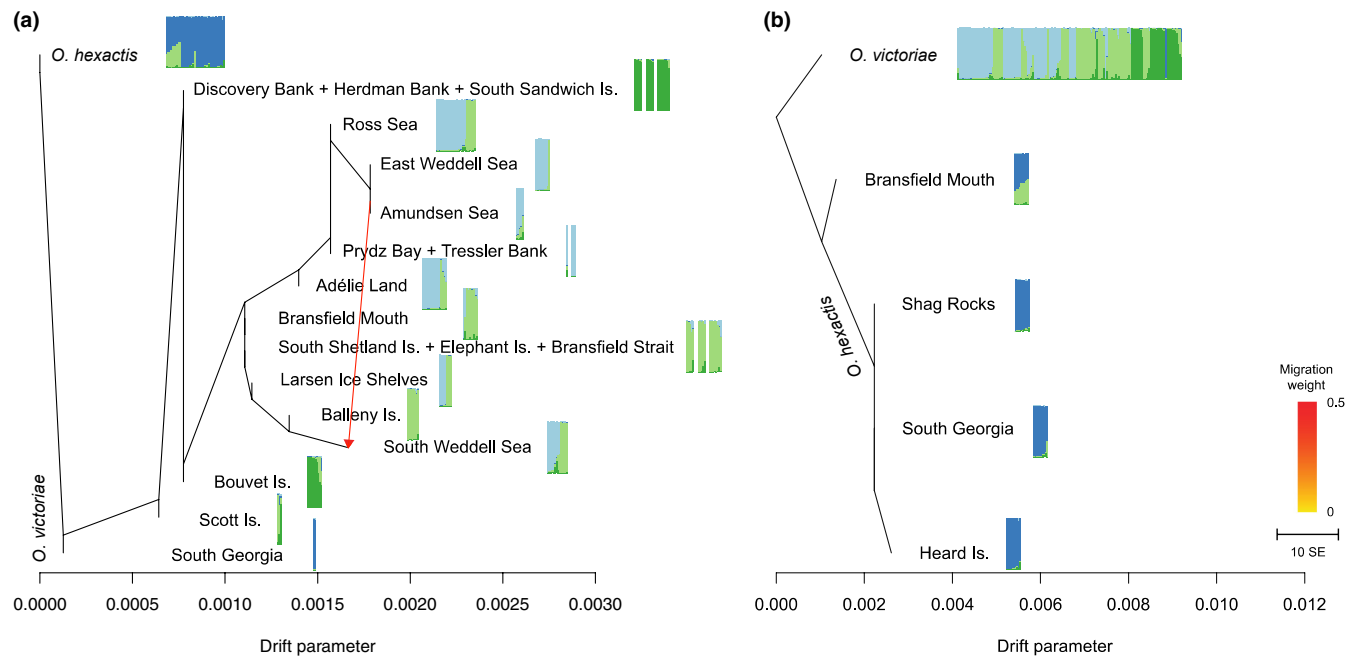

FIGURE 3 *TreeMix* maximum likelihood (ML) tree of (a) *Ophionotus victoriae* rooted with *O. hexactis* and (b) *O. hexactis* rooted with *O. victoriae*. Terminal nodes are subdivided based on neighbouring geographical locations with similar admixture proportions estimated by *Structure* (preferred *K* = 4). Horizontal branch lengths are proportional to the amount of genetic drift occurred on each branch. In the bar plots, each vertical bar represents one individual sample from the corresponding geographic location(s), with colours correspond to admixture proportion estimations. (a) Optimal migration edge of 1 (Amundsen Sea ->South Weddell Sea) was inferred by simple exponential and nonlinear least squares model and was also supported by f_4 statistic and jackknife significance test (*p* = .0005). Migration edge was coloured based on migration weight, which corresponds to the % ancestry in the sink population originated from the source population. (b) Optimal migration edge of 0 was inferred by simple exponential and nonlinear least square model and was also supported by f_4 statistic and jackknife significance test.

hexactis (Figure 3a). A migration edge of one significantly improved the model fit to the observed allele frequency data. Overall, on the ML population tree of *O. victoriae*, short internal branches with limited genetic drift were observed at each locality (Figure 3a, Appendix S1: Figure S5). Stepwise population splits were observed between Scott Island, Discovery Bank + Herdman Bank + South

Sandwich Islands (grouped together) and Bouvet Island. Samples from the Ross Sea, east Weddell Sea and Amundsen Sea formed a distinct cluster, with migration detected from the Amundsen Sea to the south Weddell Sea. Gene flow between the Amundsen Sea and the south Weddell Sea was further supported by f_4 statistics (Z-score <−3) (Table S1-S9).

Within *O. hexactis*, *TreeMix* (explained 96.7% of the total variance) revealed that this species formed two separate clades, with individuals from Bransfield Mouth grouped in a single clade, and individuals from Shag Rocks, South Georgia and Heard Island grouped in a separate clade. Overall, *O. hexactis* from Bransfield Mouth were most closely related to *O. victoriae* on the ML tree (Figure 3b, Appendix S1: Figure S13). No significant migration edge was detected within *TreeMix*. Although no admixture between populations was detected in f_3 statistics, f_4 statistics indicated gene flow either between *O. victoriae* and *O. hexactis* from Bransfield Mouth, or between Shag Rocks, South Georgia and Heard Island within *O. hexactis* (Table S1-S9).

3.4 | Environmental association analyses

When comparing *O. victoriae* and *O. hexactis* (while considering the two *O. victoriae* samples from South Georgia as *O. hexactis*) in the RDA, constrained ordination significantly explained 2.17% (adjusted R^2, $p < .001$) of the overall genetic variation with all six environmental variables. The first three constrained PC axes significantly explained 39.0%, 16.3% and 13.3% of the total adjusted R^2 ($p < .001$). On PC1 and 2, between species, *O. hexactis* showed a generally positive association with water temperature (Figure 4a). Within the RDA of *O. victoriae*, constrained

ordination significantly explained 0.88% (adjusted R^2, $p < .001$) of the overall genetic variation with five environmental variables. The first two constrained PC axes significantly explained 27.3 and 19.7% of the total adjusted R^2 ($p < .001$). On PC1 and 2, within *O. victoriae*, samples from the deep continental shelf (>1000m) exhibited a positive association with water depth, and those collected around Antarctic islands exhibited a positive association with sea surface temperature (Figure 4b). Within the RDA of *O. hexactis*, constrained ordination significantly explained 2.26% (adjusted R^2, $p < .001$) of the overall genetic variation with three environmental variables. The first three constrained PC significantly explained 40.9%, 31.1% and 28.0% of the total adjusted R^2 ($p < .05$). On PC1 and 2, samples of *O. hexactis* from the Bransfield Mouth showed a positive association with water depth, but negative associations with bottom water salinity were observed in samples from Heard Island (Figure 4c).

3.5 | Outlier loci

Based on the outlier loci detected by at least two methods (*PCAdapt*, *OutFLANK*, RDA and *BayeScan*), a total of 30, 25 and 11 loci were identified as putative outliers between species, within *O. victoriae*, and within *O. hexactis*, respectively (Appendix S1: Figure S14, Table S1-S9).
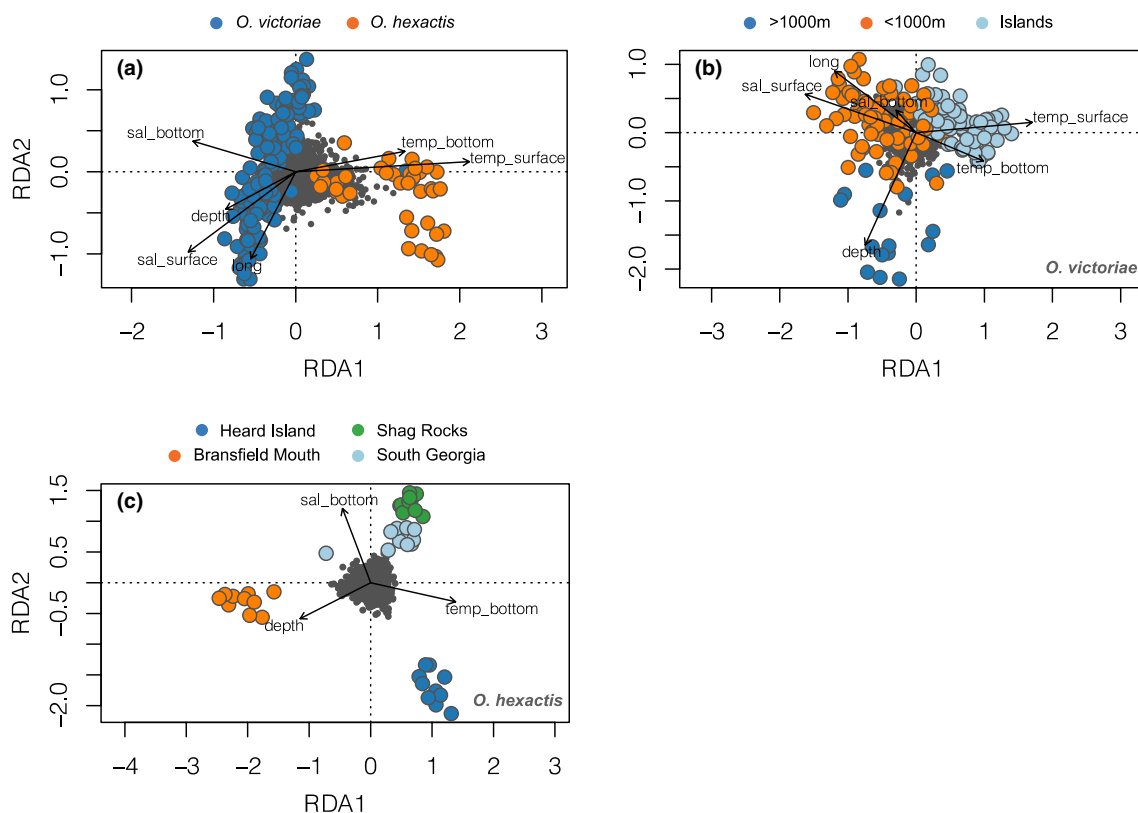

FIGURE 4 Redundancy analysis (RDA) showing genotype–environment association in *Ophionotus victoriae* and *O. hexactis* on the first two constrained axes. Grey dots represent SNPs, and coloured circles represent individual sample defined by assigned labels. Vectors represent environmental predictors, including surface water salinity (sal_surface), bottom water salinity (sal_bottom), surface water temperature (temp_surface), bottom water temperature (temp_bottom), water depth (depth). (a) Samples of *O. victoriae* and *O. hexactis* defined by species ($n = 195$, 1781 loci). (b) Samples of *O. victoriae* grouped by deep continental shelf (>1000m), shallow continental shelf (<1000m) or Antarctic islands. (c) Samples of *O. hexactis* are defined by geographical locations.

No outlier loci were matched with the BLASTx database under the search criteria. One outlier locus (Clocus-186281) detected between species was a positive match to the InterPro database with GO annotations (Ionotropic glutamate receptor, InterPro ID: IPR001320, Table S1-S9). RDA also predicted outlier loci correlated with selected environment variables on the significant constrained axes. When comparing *O. victoriae* and *O. hexactis* samples, outlier loci were correlated with bottom water salinity ($n=22$), surface water salinity ($n=16$), water depth ($n=14$), sea bottom temperature ($n=7$) and longitude ($n=3$, Table S1-S9). Within *O. victoriae*, outlier loci were correlated with water depth ($n=14$), sea surface temperature ($n=8$) and sea surface salinity ($n=5$, Table S1-S9). Within *O. hexactis*, outlier loci were correlated with bottom water temperature ($n=9$), bottom water salinity ($n=7$) and water depth ($n=4$, Table S1-S9).

3.6 | Demographic modelling between species

Upon inspecting the observed 1d SFS from *O. victoriae* and *O. hexactis* (excluding samples with strong interspecific admixture), both species are characterized by a W-shaped SFS with internal peak at intermediate frequencies; a stronger peak was observed within *O. hexactis* (Figure 5a). The observed 2d SFS between *O. victoriae* and *O. hexactis* also indicated a lack of intermediate frequencies SNPs shared between *O. victoriae and O. hexactis* (Figure 5a, b). However, these putative missing SNPs were modelled using *dadi*, leading to high residual values at sites with intermediate frequencies between observed and expected 2d SFS (Figure 5b).

Of all nine models that examined the divergence and gene flow between *O. victoriae* and *O. hexactis*, all of them returned strong and autocorrelated residuals (Figure S15). These suggest bad fits between models and observed data, therefore, we did not interpret parameter estimates further. Additionally, the optimized parameters of the model 'SI_size' returned unrealistic chi-squared values, indicating a breakdown when modelling the expected number of variants against observed data. Model ranking indicated all models involving gene flow between *O. victoriae* and *O. hexactis* were a better fit to observed data relative to models with no gene flow between species (Table S1-S9).

3.7 | Past changes in effective population size within species

Given *O. victoriae* is characterized by metapopulation structure, its rate of coalescent events would be confounded by the presence of population structure and the migration rate (Lesturgie et al., 2021; Mazet et al., 2016). Therefore, while the results of *StairwayPlot* would still be related to demographic events, care should be considered when interpreting them. In *O. victoriae*, when samples were grouped by deep-water refugia, in situ continental shelf refugia or in situ Antarctic island refugia (glacial refugia categories), a signature that resembled a 'population expansion followed by a bottleneck' was observed in the latter two categories (Figure 6a). Samples of *O. victoriae* from the deep continental shelf (deep-water refugia) were associated with a signature that resembled a 'stable population size followed by a bottleneck' (Figure 6a).

Because *O. hexactis* is characterized by panmixia, the distribution of coalescence times should be directly related to changes in population size, and therefore, results of *StairwayPlot* can be directly interpreted as realistic signals of past population size change over time (Lesturgie et al., 2021). Within *O. hexactis*, for samples from the Bransfield Mouth, *Stairwayplot* indicated a stable population size followed by a bottleneck (Figure 6b). However, a population expansion followed by a bottleneck was observed in samples from South Georgia + Shag Rocks + Heard Island (grouped together) (Figure 6b).

4 | DISCUSSION

4.1 | Genetic connectivity within *O. victoriae* (pelagic larvae)

A previous study based on mitochondrial (COI) and 2b-RAD data focusing on samples from West Antarctica suggested *O. victoriae* contains up to four distinct lineages, possibly representing multiple cryptic species (Galaska et al., 2017). A later study based on COI data focusing on samples from both West and East Antarctica suggested *O. victoriae* constitutes a single species with a circumpolar
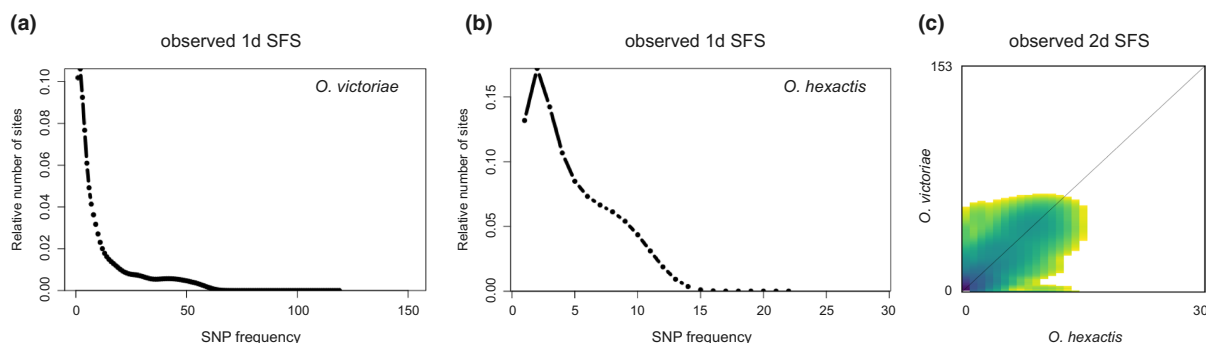

FIGURE 5 Summary of the observed frequency spectrum (SFS) of *Ophionotus victoriae* and *O. hexactis*. (a, b) One-dimensional (1d) SFS within *O. victoriae* and *O. hexactis*. (c) Folded (i.e. no outgroup data) two-dimensional (2d) SFS between *O. victoriae* and *O. hexactis*, excluding samples of *O. victoriae* from South Georgia and *O. hexactis* from Bransfield Mouth with strong interspecific admixture.
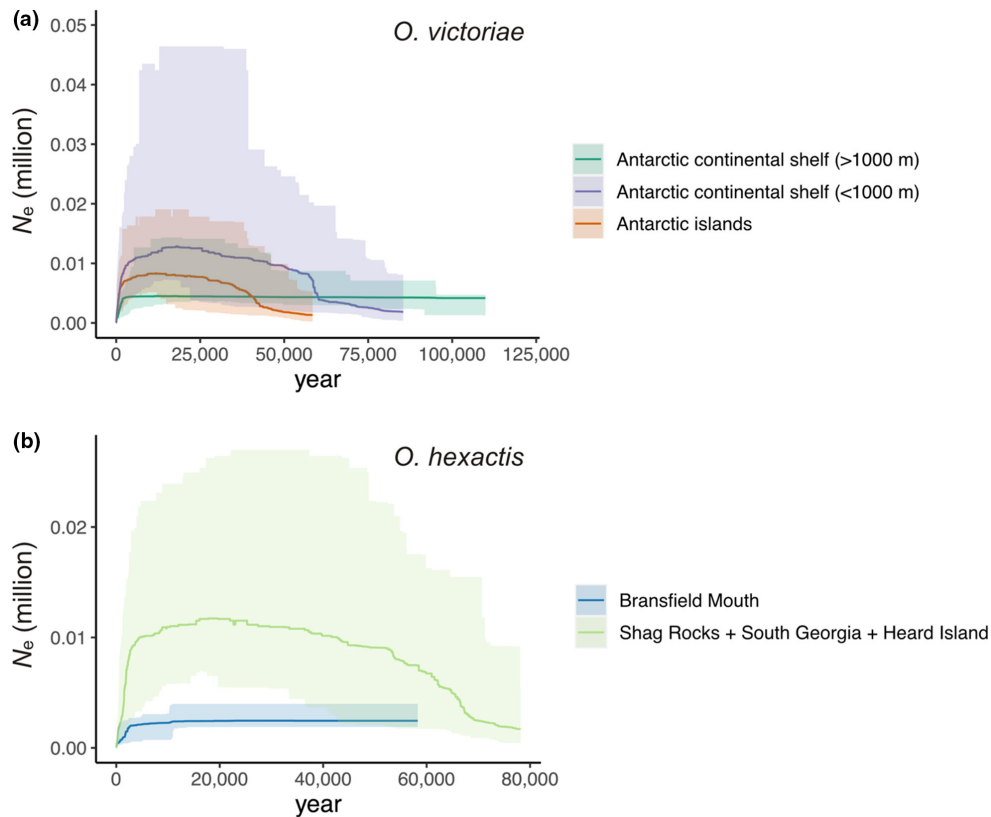
FIGURE 6 *Stairwayplot* estimates of past effective population size (N_e) changes over multiple epochs in (a) *Ophionotusvictoriae* with samples grouped by deep continental shelf (>1000m), shallow continental shelf (<1000m) and Antarctic islands and in (b) *O. hexactis* with samples grouped by geographical locations. Estimates were based on folded site frequency spectra, as well as the assumption of a mutation rate of 1.43×10^{-8} per site per generation (O'Hara et al., 2019) and a generation time of 9 years (Dahm & Brey, 1998; Grange et al., 2011). Shaded areas represent 95% confidence intervals.

distribution (Lau et al., 2021). The genomic data here also support *O. victoriae* as a single species with a circumpolar distribution containing three intraspecific admixed lineages. These lineages do not represent cryptic species as there is no disjunct differentiation within *O. victoriae* based on additional analyses (e.g. PCA and *TreeMix*).

Individual admixture proportions showed both connectivity and structure across geographical locations in *O. victoriae*, possibly linked to current dynamics and biogeography. Individual admixture proportions showed three distinct genetic clusters in *O. victoriae*, with clear isolation of genetic clusters 1, 2 and 3 (of $K=3$) observed across the vast Southern Ocean. Specifically, Antarctic island locations near the Polar Front (South Georgia, Discovery Bank, Herdman Bank, South Sandwich Islands and Bouvet Island) are distinctly associated with cluster 3 (of $K=3$), with some individuals from Bouvet Island also exhibiting admixture with cluster 2. Cluster 2 (of $K=3$) reflects circumpolar connectivity between the Antarctic continental shelf, Scotia Sea and Antarctic islands. Many of the island locations of cluster 2 coincide with the southern boundary of the ACC (sbACC) (Sokolov & Rintoul, 2009). The biogeography of cluster 2 in the central Scotia Sea, Larsen Ice shelf and south Weddell Sea also coincides with the circulation

pattern of Antarctic coastal current that connects these locations (Collares et al., 2018). Similar gene flow patterns related to the Antarctic coastal current has been reported in the Antarctic bivalve *Aequiyoldia eightsii* (Muñoz-Ramírez et al., 2020). The presence of cluster 2 in the Ross Sea also suggests a relationship between sbACC and the Ross Gyre in larval dispersal. Although the sbACC does not penetrate through the Ross Sea, it connects to the contours of the Ross Gyre (Dotto et al., 2018). The Ross Gyre is a cyclonic regional gyre in the Southern Ocean that connects the ACC to the Ross Sea continental shelf, which would explain the presence of cluster 2 connecting Adélie Land, the Balleny Islands, Scott Island and the Ross Sea.

Finally, cluster 3 (of $K=3$) is mostly observed around the Antarctic continental shelf (with one exception individual in Bransfield Mouth), suggesting genetic homogeneity around the shelf. Connectivity around the Antarctic continental shelf has also been observed in other Southern Ocean benthic species linking to the ACC (Hemery et al., 2012; Matschiner et al., 2009; Raupach et al., 2010; Sands et al., 2015; Sands et al., 2021). Alternatively, such circularity could also be linked to the eastward-flowing Antarctic Slope Current (Thompson et al., 2018).

4.2 | Genetic connectivity within *O. hexactis* (brooded juveniles)

For *O. hexactis*, a distinct population structure was observed in Bransfield Mouth, and panmixia was observed across other localities (South Georgia, Shag Rocks and Heard Island). Significant differentiation was also detected between all locations, however, strong gene flow (inferred from panmixia) was also observed among South Georgia, Shag Rocks and Heard Island, even though some of these locations are separated by the long geographical distance around the Southern Ocean. Signatures of panmixia in *O. hexactis* is likely linked to gene flow rather than asexual reproduction. While asexual reproduction (via fission) is common among hexamerous ophiuroids, it is understood that brooding (sexual reproduction) does not co-occur with fissiparity in ophiuroids (Stöhr et al., 2012). A previous study also reported that *O. hexactis* is an intraovarian brooder (Turner & Dearborn, 1979). Together, the evidence suggests both long-distance dispersal and genetic isolation are possible for Southern Ocean benthic species with a brooding strategy.

Previous studies have highlighted that Southern Ocean benthic brooders can be characterized by geographic structure due to their limited dispersal ability across the vast Southern Ocean (Moreau et al., 2017, 2019). However, most of the existing genetic evidence outlining distinct segregated population structures in Southern Ocean brooding species or species with benthic hatchings are linked to the islands within the Scotia Sea (Hoffman et al., 2011; Linse et al., 2007; Strugnell et al., 2017). Additionally, it has been argued that some brooding species exhibit genetic connectivity across the Southern Ocean (reviewed by Halanych and Mahon (2018)). For *O. hexactis* around West Antarctica, it appears that locations across the Scotia Arc are highly separated, indicating that the Scotia Arc system could promote genetic isolation and diversification, as suggested for other Southern Ocean species (Demarchi et al., 2010; Hoffman et al., 2011; Linse et al., 2007; Verheye et al., 2016). However, the barriers across the Scotia Arc are permeable, as one *O. hexactis* sample from South Georgia also falls within the genetic cluster distinct to Bransfield Mouth.

Beyond the Bransfield Strait, individuals sampled around South Georgia, Shag Rocks and Heard Island were associated with long-distance connectivity. To date, the only proposed pathway for long-distance dispersal in Antarctic benthic invertebrates with a brooding strategy is via a kelp raft along the ACC (e.g. Nikula et al., 2010). The maximum disc diameter of *Ophionotus hexactis* is ~39 mm (Grange et al., 2004), and the size of *O. hexactis* suggests that it can possibly reside within the holdfast of a kelp raft. However, this species is mostly found in a flat muddy bottom, between ~0 and 300 m, which is not the habitat for kelp. They do not typically wrap their arms around substrates that may raft, and this species has never been found on kelp rafts before. More importantly, the *O. hexactis* samples that were collected in this study were from 119 to 302 m that are out of reach by algal rafts. Nonetheless, long-distance dispersal signals are apparent, although the mechanism by which they disperse is not yet identified.

4.3 | Genomic signatures of Southern Ocean glacial cycle survival

4.3.1 | Deep-water refugia in O. victoriae

During Pleistocene glacial maxima, the deep seafloor of the Southern Ocean was not impacted by the continentally grounded ice sheets. The large deep-sea habitable area was hypothesized to enable refugial populations to persist, maintain and/or expand in size and diversify (Allcock & Strugnell, 2012). In *O. victoriae*, a strong genotype–environmental association with depth was observed in deep-water samples (>1000 m), suggesting isolation-by-water depth. Isolation-by-depth is expected when populations have been stable over time, spatially neighbouring populations are more genetically similar to each other than distant neighbours, and diverging populations are isolated by selective forces on ecology and reproductive barriers (Wright, 1943). The strong genotype association with depth is likely linked to long-term diversification within deep-water refugi.

Stairwayplot indicates deep-water samples (>1000 m) exhibit a distinctly different demographic history compared to shallow continental shelf (<1000 m) and Antarctic island samples. *O. victoriae* is characterized by a metapopulation structure, meaning that demographic signatures captured by *Stairwayplot* would be confounded by population structure and migration rate. Even when considering the impact of metapopulation on coalescence times, the signature that resembles a 'stable population size followed by a bottleneck' observed in deep-water samples (>1000 m) would likely be driven by a low migration rate or time of recent colonization associated with a high migration rate (Lesturgie et al., 2021). Either explanation fits within the hypothesis of deep-sea refugia for *O. victoriae*. The scenario of a low migration rate would indicate a signature of an independent deep-sea refuge; alternatively, the time of recent colonization associated with a high migration rate would indicate retreat into deep-sea refugia only if it occurred in recent time, likely the Last Glacial Maximum.

Signatures of deep-water refugia likely represent a single connected refugium. Samples of *O. victoriae* from the deep continental shelf (>1000 m) are observed in sites that are separated by long distances (Ross Sea, Adélie Land, Amundsen Sea, south Weddell Sea). If deep-water refugia were geographically structured within *O. victoriae*, isolation-by-distance and subsequent genetic drift would be expected to create a distinct structure. When samples of *O. victoriae* from >1000 m were analysed together, limited genetic differentiation was observed between them (PCA). Strong signals of deep-water refugia characteristics were also highlighted by separate analyses (RDA, Stairway Plot). So far, the evidence supports a single connected deep refugium.

4.3.2 | In situ shelf and island refugia

Even during the most extreme glacial maxima (e.g. LGM), where the grounded ice from the AIS eroded most of the continental shelf habitat, pockets of ice-free areas have been proposed to exist along

the continental shelf edge as well as around some Antarctic islands (Thatje et al., 2005). In situ refugia in the Southern Ocean were hypothesized to enable small populations to persist throughout glacial cycles and would be characterized by signatures of bottlenecks followed by population expansion (Allcock & Strugnell, 2012). For *O. victoriae*, the overall negative neutrality tests (all sequences pooled) suggest that this species experienced a population bottleneck followed by expansion.

Genetic structure distinct to either the continental shelf or Antarctic islands was observed within *O. victoriae*, likely further supporting the hypothesis of independent continental shelf and Antarctic island in situ glacial refugia. However, the location-specific structure was not detected, likely due to the low and uneven sample size between locations. Therefore, the exact locations of in situ glacial refugia cannot yet be pinpointed.

Incorporating the influence of metapopulation structure on *StairwayPlot* results, following simulations within Lesturgie et al. (2021), *StairwayPlot* further supported the scenario of historical colonization with high gene flow between locations in samples from shallow continental shelf sites (<1000 m) and around Antarctic islands. The concept of historical colonization further supports the hypothesis of in situ refugia; as grounded ice sheets retreated following the end of glacial maxima (e.g. LGM), refugial populations likely recolonized ice-free areas after deglaciation (Thatje et al., 2005). Given the confounding factors linked to metapopulation structure, the dating of demographic histories would not reflect the exact dates of recolonization and in situ refugia, however, the retrieved timing of events should be consistent relative to each other (Lesturgie et al., 2021). At least in *O. victoriae*, a signature of 'population expansion' and the most recent common ancestor (TMRCA) was observed to be older in samples from shallow continental shelf sites (<1000 m), suggesting demographic processes associated with in situ refugia likely emerged around the Antarctic continental shelf first, followed by habitats around Antarctic islands.

After the LGM, refugial populations likely recolonized ice-free areas after deglaciation (Thatje et al., 2005) but the extent and pathways of recolonization remain unclear. In *O. victoriae*, the clear gene flow and some admixture observed between locations, suggest recolonization could have been widespread across the continental shelf and Antarctic islands. The pathways of recolonization could have been driven by oceanic currents leading to present-day genetic patterns (see above), and each location could have received migrants from refugial populations.

For *O. hexactis*, signatures of in situ refugia were detected around Antarctic Islands. Negative neutrality tests and *StairwayPlot* indicate population bottlenecks at all sampled locations, suggesting signatures of in situ refugial survival. Samples from the Bransfield Mouth were characterized by stable population structure between ~60 and ~10 kya, followed by population bottlenecks at ~10 kya, as well as association with water depth. Samples from Shag Rocks, South Georgia and Heard Island were characterized by an increase in population size since ~80 kya, followed by population bottlenecks

at ~18 kya. The distinctly different demographic histories observed between Bransfield Mouth vs Shag Rocks, South Georgia and Heard Island suggest independent in situ glacial refugia associated with respective environments. Ice sheet reconstructions also indicate areas where *O. hexactis* could have found refuge (Bransfield Mouth, Shag Rocks and Heard Island) that were not (or only partially) impacted by grounded ice (Hodgson et al., 2014; Simms et al., 2011), further supporting the case of in situ refugia in these areas.

4.4 | Inferring demographic histories from alleles shared between *O. victoriae* and *O. hexactis*

The overall genomic data suggest apparent gene flow between *O. victoriae* and *O. hexactis*, despite clear morphological, life history and allelic differences between them. Some *O. victoriae* individuals from Bransfield Mouth, and all individuals from South Georgia, show evidence of admixture with *O. hexactis* where their distribution overlaps. The sequenced *O. victoriae* specimens from South Georgia are unlikely to be *O. hexactis* as they exhibit typical taxonomic features (5 arms) of this species (examined by Lau et al., 2021). At each of the three most differentiated loci contributing to the discriminant functions, *O. victoriae* from South Georgia shared similar major and minor allele frequencies with *O. hexactis*, and *O. hexactis* from Bransfield Mouth also shared similar major and minor allele frequencies with *O. victoriae*. Distinctly different interspecific admixture signals were observed at the Bransfield Mouth and South Georgia, possibly indicating independent occasions (over time and/or across spatial scale) of gene flow between species in areas where they overlap.

To explore the broad relationship between species, we excluded samples with interspecific admixture (*O. victoriae* from South Georgia and *O. hexactis* from Bransfield Mouth) for SFS-based demographic analyses. First, the observed 2d SFS indicated limited alleles at intermediate frequencies were shared between *O. victoriae* and *O. hexactis*. This is likely a true biological signal, as our target capture method captures nonvariable ddRAD loci that would be present across *Ophiontous victoriae* and *O. hexactis* (which rules out ascertainment bias), and we also examined our dataset with a genotype likelihood estimation approach (which excludes potential sequencing errors due to low coverage). However, it is possible that bioinformatic errors may exist and that we are unable to identify them. Due to such extreme allelic differences between species, *dadi* residuals of fitted models were strong and autocorrelated, suggesting all tested models were a poor fit to the observed data. Additionally, a more complex population structure may exist between and within *O. victoriae* and *O. hexactis* that could have contributed to the poor fit of *dadi*-modelled data against observed data. Instead of focusing on interpreting parameter estimates recovered, we discuss the broadly concordant patterns observed from tested models to explore species relationships.

Among the tested demographic models, all models involving gene flow between *O. victoriae* and *O. hexactis* were ranked higher than the models involving strict isolation between species. Furthermore,

all models involving gene flow between species suggested a higher number of migrants per generation from *O. victoriae* to *O. hexactis*, suggesting opportunities for admixture could be greater in one direction than the other. Sperm chemotaxis (sperm attraction towards eggs) is generally species specific in ophiuroids and has been linked to reproductive isolation in closely-related ophiuroid species with contrasting reproductive strategies (brooding vs broadcasting) (Weber et al., 2017). Even though sperm chemotaxis has not been examined in Antarctic ophiuroids, it is unlikely that there is a species-specific barrier between *O. victoriae* and *O. hexactis*, given the apparent gene flow and admixture observed. The higher proportion of gene flow from *O. victoriae* to *O. hexactis* could be related to a higher number of gametes (sperm and eggs) associated with *O. victoriae* compared to *O. hexactis* being made available for cross-fertilization. For example, in a reproductive season, a single female *O. victoriae* releases 100,000–160,000 eggs (a broadcast spawner) (Grange et al., 2004), whereas a single *O. hexactis* female releases an average brood size of 24 juveniles (Turner & Dearborn, 1979).

4.5 | Lack of alleles at intermediate frequencies shared between *O. victoriae* and *O. hexactis*

The observed 1d SFS of both species are associated with a peak at intermediate frequencies across genome-wide data (W-shaped SFS). The alleles associated with this peak appear to be species specific, and the intermediate-frequency variants are far more excessive in *O. hexactis*. W-shaped SFS could be linked to a high admixture rate (>0.2) with more than one ancestral allele being introduced at previously fixed sites (Marchi & Excoffier, 2020). This is unlikely as the overall genomic data so far do not suggest such strong recent admixture between species. W-shaped SFS could also be linked to a recent bottleneck (discussed within Charlesworth & Jain, 2014). However, both *O. victoriae* and *O. hexactis* persisted in in situ Antarctic islands refugia with bottlenecks, yet *O. hexactis* is characterized with far more excessive number of intermediate-frequency variants. Additionally, *O. hexactis* persisted in in situ Antarctic island refugia that are near the Polar Front, and these islands were not (or only partially) impacted by grounded ice during the LGM (Hodgson et al., 2014; Simms et al., 2011). Therefore, *O. hexactis* would not have experienced an extreme bottleneck in the recent past, and overall, a bottleneck does not seem to explain the W-shaped SFS in *O. hexactis*.

Alternative explanations of a W-shaped SFS in *O. hexactis* include balancing selection (Cheng & Degiorgio, 2020) and associative overdominance (heterozygous advantage at neutral loci) (Gilbert et al., 2020) on standing genetic variation, both of which could be linked to recent adaptation (Dragh & Whilock, 2014; Kelly & Hughes, 2019). For the case of *O. hexactis*, the observed genome-wide excess of intermediate-frequency alleles clearly departs from neutrality, and we hypothesize that it could too be driven by recent adaptation, and the most apparent adaptation in *O. hexactis* is the switch to brooding and an increase in arm number.

4.6 | What drove evolutionary innovation in *O. hexactis* (switch to brooding and an increase in arm number)?

Within *O. hexactis*, *StairwayPlot* indicated that TMRCA could be traced back to ~78 ka. This time estimate is unlikely to reflect the divergence time of *O. hexactis*, as previous exon data suggested *O. victoriae* and *O. hexactis* diverged at ~1.64 mya (95% confidence interval 0.53–5.79 mya) (O'Hara et al., 2017). Nonetheless, the TMRCA in *O. hexactis* observed in this study could shed light on the events linked to evolutionary innovations (i.e. potential drivers of the genome-wide excess in intermediate-frequency alleles). For example, *O. hexactis* likely persisted in situ around Antarctic islands at relatively shallow depths throughout the late Pleistocene. The Antarctic Ice Sheet likely retreated significantly in recent interglacials during the late Pleistocene (Dutton et al., 2015), which would result in low-salinity outflow towards the upper Southern Ocean (Jacobs et al., 1996). Therefore, the innovation of six arms and brooding within *O. hexactis* could have been influenced by the low-salinity meltwater, given that this species would have been directly exposed to glacial meltwater. Supporting this concept, environmental association analysis (RDA) also detected 61% of the outlier loci as being linked to salinity. However, we only sampled a few loci via a reduced representation approach, and the W-shaped SFS in both species clearly indicates that their demographic history deviates from expected neutrality; ultimately, the possible associations of outliers with the phenotypic differences remain to be tested further.

In brittle stars, increased arm numbers are related to water-pumping motions of solid matter transport, escape strategies and coordination (Clark, Fezzaa, et al., 2019; Clark, Kanauchi, et al., 2019; Wakita et al., 2019, 2020). The decentralized nervous system in brittle stars also means that any arm can act as the responsive leading arm upon stimulus, thus individuals with a higher number of arms (six or seven) can lead to a more random escape pattern compared to five arms (Wakita et al., 2020). Arm numbers are also positively related to coordinated locomotion in brittle stars (Clark, Kanauchi, et al., 2019). In this study, one of the outlier loci identified between *O. hexactis* and *O. victoriae* matched with the protein-coding gene of ionotropic glutamate receptors. Although the function of the ionotropic glutamate receptors is not fully understood, in echinoderms, this receptor has been found to be a chemoreceptor gene within the olfactory organs of a crown-of-thorns starfish (Roberts et al., 2018), and responsible for arm autotomy in the crinoid *Antedon mediterranea* (Wilkie et al., 2010). Arm autotomy is a common defensive process in ophiuroids in response to threats (Clark, Fezzaa, et al., 2019). Similarly, *O. victoriae* is also known to exhibit a high degree of arm autotomy (as well as a lack of feeding response) when under stress in captivity (Fratt & Dearborn, 1984). Although only one annotated gene was found to be an outlier in *O. hexactis*, the increase in arm number in this species, based on all the benefits discussed above, could reflect ecological specialization such as response and movement coordination, within the fluctuating environment throughout the late Pleistocene.

Finally, in echinoderms, brooding has often emerged under stressful environmental conditions during lineage transition over macroevolutionary time frames (Lawrence & Herrera, 2000), even though this strategy requires higher maternal investment compared with pelagic larval development (Fernández et al., 2000). There is an unusually high proportion of echinoderms with brooding relative to broadcast spawning strategies in the Southern Ocean (Poulin & Féral, 1996). Brooding is also prevalent among ophiuroids in the Southern Ocean. In particular, Mortensen (1936, in Pearse et al., 2009) estimated that ~50% of Antarctic and sub-Antarctic ophiuroids are brooders. The prevalence of brooding in Southern Ocean echinoderms is likely not an adaptation to current polar environmental conditions, but rather linked to events in the past (Pearse et al., 2009). Brooding could also reflect a general adaptation to the lack of primary productivity and limited habitat availability for successful pelagic larval development during glacial cycles (Poulin et al., 2002).

Emerging evidence has also highlighted that contrasting life histories can be found between closely-related ophiuroid species in the Southern Ocean, with brooding strategies mainly found around Antarctic islands and broadcasting strategies mainly observed on the Antarctic continental shelf (Jossart et al., 2019; Sands et al., 2021; this study). For example, there are strong parallels in the case of 5 vs 6 arms and brooding vs broadcasting between *Ophiontous* and *Ophiosabine* (Sands et al., 2021). Brooding and broadcasting in congeneric species have also been reported in other extant echinoderms in the Southern Ocean, including the *Astrotoma agassizii* complex (Jossart et al., 2019). It is likely that some of the genomic signatures observed in this study, such as an excess of intermediate-frequency alleles could be extended to other ophiuroid species with similar evolutionary histories as *Ophionotus*.

5 | CONCLUSION

We found that *O. victoriae* and *O. hexactis* are closely-related species with interspecific gene flow detected in overlapping locations of their distribution. The genome-wide data also revealed multiple evolutionary forces likely influencing population genetic patterns in the Southern Ocean. The genetic structure of *O. victoriae* indicate the impact of glacial cycles, such as survival in in situ shelf refugia and deep-water refugia, may have played a major role in shaping the present-day distribution and genetic structure of *O. victoriae*. In addition, while the ACC is discussed as the main driver of circumpolar genetic connectivity in *O. victoriae*, local current dynamics may also structure the species' connectivity patterns regionally. The genetic pattern of *O. hexactis* is likely driven by the combination of glacial refugia survival and oceanic currents. Panmixia was observed between West and East Antarctica, with distinct genetic structure observed within the Bransfield Mouth in the Scotia Arc.

Both *O. victoriae* and *O. hexactis* are associated with an SFS with a W-shaped peak in alleles observed at intermediate frequencies; the alleles associated with this peak appear to be species specific,

and these intermediate-frequency variants are far more excessive in *O. hexactis*. We evaluate the ecological drivers behind the evolutionary innovations in *O. hexactis* (increase in arm number and a switch to brooding from broadcasting) and hypothesise that the peak in alleles at an intermediate frequencies could be related to recent adaptation, linked to evolutionary innovations. There are strong parallels in the case of 5 vs 6 arms and brooding vs broadcasting between closely-related ophiuroid species in the Southern Ocean, and further whole-genome studies should focus on examining the relationship between evolutionary innovation and genome-wide selection.

AUTHOR CONTRIBUTIONS
J.M.S. and N.G.W. designed the research. N.G.W. and C.J.S. provided biological samples. S.C.Y.L, J.M.S., C.N.N.S. and N.G.W. developed sequencing strategies. S.C.Y.L. analysed the data. J.M.S., C.N.N.S. and N.G.W. supervised data analyses. S.C.Y.L. wrote the original draft. J.M.S., C.N.N.S., C.J.S. and N.G.W. reviewed and edited the manuscript.

CONFLICT OF INTEREST STATEMENT
The authors declare that they have no conflict of interests.

OPEN RESEARCH BADGES

This article has earned an Open Data badge for making publicly available the digitally-shareable data necessary to reproduce the reported results. The data is available at https://github.com/sallycylau/ophionotus_ddRADcapture.

DATA AVAILABILITY STATEMENT

Raw ddRADseq sequences relevant to the ddRAD loci discovery of Antarctic brittle stars *Ophionotus victoriae* and *O. hexactis* are deposited in the SRA BioProject PRJNA882200. Raw sequences relevant to the target capture sequencing of ddRAD loci in *O. victoriae* and *O. hexactis* are deposited in the SRA BioProject PRJNA883508. Scripts to reproduce all analyses in this study are available in Github at https://github.com/sallycylau/ophionotus_ddRADcapture.

BENEFIT-SHARING STATEMENTS

Benefit Generated: Benefits from this research accrue from the sharing of our data and results on public databases as described above.

ORCID

Sally C. Y. Lau https://orcid.org/0000-0002-4955-2530
Jan M. Strugnell https://orcid.org/0000-0003-2994-637X
Chester J. Sands https://orcid.org/0000-0003-1028-0328
Catarina N. S. Silva https://orcid.org/0000-0001-9401-2616
Nerida G. Wilson https://orcid.org/0000-0002-0784-0200

REFERENCES

Agarwala, R., Barrett, T., Beck, J., Benson, D. A., Bollin, C., Bolton, E., Bourexis, D., Brister, J. R., Bryant, S. H., Canese, K., Cavanaugh, M., Charowhas, C., Clark, K., Dondoshansky, I., Feolo, M., Fitzpatrick, L., Funk, K., Geer, L. Y., Gorelenkov, V., … Zbicz, K. (2018). Database resources of the National Center for biotechnology information. *Nucleic Acids Research*, 46, D8–D13. https://doi.org/10.1093/nar/gkx1095

Allcock, A. L., & Strugnell, J. M. (2012). Southern Ocean diversity: New paradigms from molecular ecology. *Trends in Ecology and Evolution*, 27, 520–528. https://doi.org/10.1016/j.tree.2012.05.009

Altschul, S. F., Gish, W., Miller, W., Myers, E. W., & Lipman, D. J. (1990). Basic local alignment search tool. *Journal of Molecular Biology*, 215, 403–410. https://doi.org/10.1016/S0022-2836(05)80360-2

Anderson, J. B., Shipp, S. S., Lowe, A. L., Wellner, J. S., & Mosola, A. B. (2002). The Antarctic ice sheet during the last glacial maximum and its subsequent retreat history: A review. *Quaternary Science Reviews*, 21, 49–70. https://doi.org/10.1016/S0277-3791(01)00083-X

Andrews, S. (2010). FastQC: A quality control tool for high throughput sequence data. *Babraham Institute*. Available at: http://www.bioinformatics.babraham.ac.uk/projects/fastqc

Arnold, M. L., & Kunte, K. (2017). Adaptive genetic exchange: A tangled history of admixture and evolutionary innovation. *Trends in Ecology and Evolution*, 32, 601–611. https://doi.org/10.1016/j.tree.2017.05.007

Arnone, M. I., Byrne, M., & Martinez, P. (2015). Echinodermata. In A. Wanninger (Ed.), *Evolutionary developmental biology of invertebrates 6*. Springer Vienna.

Balaško, M. K., Nažok, R., Mikac, K. M., Benítez, H. A., Suazo, M. J., Viana, J. P. G., Lemic, D., & Živković, I. P. (2022). Population genetic structure and geometric morphology of codling moth populations from different management systems. *Agronomy*, 12, 1278. https://doi.org/10.3390/agronomy12061278

Blum, M., Chang, H. Y., Chuguransky, S., Grego, T., Kandasaamy, S., Mitchell, A., Nuka, G., Paysan-Lafosse, T., Qureshi, M., Raj, S., Richardson, L., Salazar, G. A., Williams, L., Bork, P., Bridge, A., Gough, J., Haft, D. H., Letunic, I., Marchler-Bauer, A., … Finn, R.

D. (2021). The InterPro protein families and domains database: 20 years on. *Nucleic Acids Research*, 49, D344–D354. https://doi.org/10.1093/nar/gkaa977

Boissin, E., Stöhr, S., & Chenuil, A. (2011). Did vicariance and adaptation drive cryptic speciation and evolution of brooding in *Ophioderma longicauda* (Echinodermata: Ophiuroidea), a common atlanto-mediterranean ophiuroid? *Molecular Ecology*, 20, 4737–4755. https://doi.org/10.1111/j.1365-294X.2011.05309.x

Brey, T., Dahm, C., Gorny, M., Klages, M., Stiller, M., & Arntz, W. E. (1996). Do Antarctic benthic invertebrates show an extended level of eurybathy? *Antarctic Science*, 8, 3–6. https://doi.org/10.1017/S0954102096000028

Broad Institute. (2019). Picard toolkit. *GitHub Repository*. Available at: https://broadinstitute.github.io/picard/

Catchen, J., Hohenlohe, P. A., Bassham, S., Amores, A., & Cresko, W. A. (2013). Stacks: An analysis tool set for population genomics. *Molecular Ecology*, 22, 3124–3140. https://doi.org/10.1111/mec.12354

Charlesworth, B., & Jain, K. (2014). Purifying selection, drift, and reversible mutation with arbitrarily high mutation rates. *Genetics*, 198, 1587–1602. https://doi.org/10.1534/genetics.114.167973

Chen, S., Zhou, Y., Chen, Y., & Gu, J. (2018). Fastp: an ultra-fast all-in-one FASTQ preprocessor. *Bioinformatics*, 34, i884–i890. https://doi.org/10.1093/bioinformatics/bty560

Cheng, X., & Degiorgio, M. (2020). Flexible mixture model approaches that accommodate footprint size variability for robust detection of balancing selection. *Molecular Biology and Evolution*, 37, 3267–3291. https://doi.org/10.1093/molbev/msaa134

Clark, E. G., Fezzaa, K., Burke, J. E., Racicot, R. A., Shaw, J. O., Westacott, S., & Briggs, D. E. G. (2019). A farewell to arms: Using X-ray synchrotron imaging to investigate autotomy in brittle stars. *Zoomorphology*, 138, 419–424. https://doi.org/10.1007/s00435-019-00451-7

Clark, E. G., Kanauchi, D., Kano, T., Aonuma, H., Briggs, D. E. G., & Ishiguro, A. (2019). The function of the ophiuroid nerve ring: How a decentralized nervous system controls coordinated locomotion. *Journal of Experimental Biology*, 222, jeb192104. https://doi.org/10.1242/jeb.192104

Clarke, A., & Johnston, N. M. (2003). Antarctic marine benthic diversity. In R. N. Gibson & R. J. A. Atkinson (Eds.), *Oceanography and marine biology. An annual review* (Vol. 41, pp. 47–114). CRC Press. https://doi.org/10.1201/9780203180570

Collares, L. L., Mata, M. M., Kerr, R., Arigony-Neto, J., & Barbat, M. M. (2018). Iceberg drift and ocean circulation in the northwestern Weddell Sea, Antarctica. *Deep-Sea Research Part II: Topical Studies in Oceanography*, 149, 10–24. https://doi.org/10.1016/j.dsr2.2018.02.014

Convey, P., Stevens, M. I., Hodgson, D. A., Smellie, J. L., Hillenbrand, C. D., Barnes, D. K. A., Clarke, A., Pugh, P. J. A., Linse, K., & Cary, S. C. (2009). Exploring biological constraints on the glacial history of Antarctica. *Quaternary Science Reviews*, 28, 3035–3048. https://doi.org/10.1016/j.quascirev.2009.08.015

Crame, J. A. (1997). An evolutionary framework for the polar regions. *Journal of Biogeography*, 24, 1–9. https://doi.org/10.1111/j.1365-2699.1997.tb00045.x

Crame, J. A. (2018). Key stages in the evolution of the Antarctic marine fauna. *Journal of Biogeography*, 45, 986–994. https://doi.org/10.1111/jbi.13208

Daane, J. M., Dornburg, A., Smits, P., Mac Guigan, D. J., Hawkins, M. B., Near, T. J., Dentrich, H. W., III, & Harris, M. P. (2019). Historical contingency shapes adaptive radiation in Antarctic fishes. *Nature Ecology & Evolution*, 3, 1102–1109. https://doi.org/10.1038/s41559-019-0914-2

Dahm, C., & Brey, T. (1998). Determination of growth and age of slow growing brittle stars (Echinodermata: Ophiuroidea) from natural

growth bands. *Journal of the Marine Biological Association of the United Kingdom*, *78*, 941–951. https://doi.org/10.1017/s002531540 0044891

Davidson, P. L., Guo, H., Swart, J. S., Massri, A. J., Edgar, A., Wang, L., Berrio, A., Devens, H. R., Koop, D., Cisternas, P., Zhang, H., Zhang, Y., Byrne, M., Fan, G., & Wray, G. A. (2022). Recent reconfiguration of an ancient developmental gene regulatory network in *Heliocidaris* Sea urchins. *Nature Ecology & Evolution*, *6*, 1907–1920. https://doi.org/10.1038/s41559-022-01906-9

De Broyer, C., Danis, B., Louise, A., Martin, A., Claudia, A., Tom, A., David, B., Marthan, B., Kasia, B. S., Magda, B., Jens, B., Nunes, B. S., Angelika, B., Bruno, D., Bruno, D., De Claude, B., de Miguel, S., Marc, E., Christian, E., … Wolfgang, Z. (2011). How many species in the Southern Ocean? Towards a dynamic inventory of the Antarctic marine species. *Deep-Sea Research Part II: Topical Studies in Oceanography*, *58*, 5–17. https://doi.org/10.1016/j.dsr2.2010.10.007

Demarchi, M., Chiappero, M. B., Tatián, M., & Sahade, R. (2010). Population genetic structure of the Antarctic ascidian *Aplidium falklandicum* from scotia arc and South Shetland Islands. *Polar Biology*, *33*, 1567–1576. https://doi.org/10.1007/s00300-010-0848-2

Dotto, T. S., Naveira Garabato, A., Bacon, S., Tsamados, M., Holland, P. R., Hooley, J., Frajka-Williams, E., Ridout, A., & Meredith, M. P. (2018). Variability of the Ross gyre, Southern Ocean: Drivers and responses revealed by satellite altimetry. *Geophysical Research Letters*, *45*, 6195–6204. https://doi.org/10.1029/2018G L078607

Dragh, J., & Whilock, M. C. (2014). Overdominance interacts with linkage to determine the rate of adaptation to a new optimum. *Journal of Evolutionary Biology*, *28*, 95–104. https://doi.org/10.1111/jeb.12547

Dutton, A., Carlson, A. E., Long, A. J., Milne, G. A., Clark, P. U., DeConto, R., Horton, B. P., Rahmstorf, S., & Raymo, M. E. (2015). Sea-level rise due to polar ice-sheet mass loss during past warm periods. *Science*, *349*, aaa4019. https://doi.org/10.1126/science.aaa4019

Earl, D. A., & Von Holdt, B. M. (2012). STRUCTURE HARVESTER: A website and program for visualizing STRUCTURE output and implementing the Evanno method. *Conservation Genetics Resources*, *4*, 359–361. https://doi.org/10.1007/s12686-011-9548-7

Erwin, D. H. (2021). A conceptual framework of evolutionary novelty and innovation. *Biological Reviews*, *96*, 1–15. https://doi.org/10.1111/brv.12643

Fernández, M., Bock, C., & Pörtner, H.-O. (2000). The cost of being a caring mother: The ignored factor in the reproduction of marine invertebrates. *Ecology Letters*, *3*(6), 487–494.

Fitak, R. R. (2021). OptM: Estimating the optimal number of migration edges from Treemix. *Biology Methods and Protocols*, *6*, pbab017. https://doi.org/10.1093/biomethods/bpab017

Foll, M., & Gaggiotti, O. (2008). A genome-scan method to identify selected loci appropriate for both dominant and codominant markers: A Bayesian perspective. *Genetics*, *180*, 977–993. https://doi.org/10.1534/genetics.108.092221

Forester, B. R., Lasky, J. R., Wagner, H. H., & Urban, D. L. (2018). Comparing methods for detecting multilocus adaptation with multivariate genotype–environment associations. *Molecular Ecology*, *27*, 2215–2233. https://doi.org/10.1111/mec.14584

Fratt, D. B., & Dearborn, J. H. (1984). Feeding biology of the Antarctic brittle star *Ophionotus victoriae* (Echinodermata: Ophiuroidea). *Polar Biology*, *3*, 127–139. https://doi.org/10.1007/BF00442644

Galaska, M. P., Sands, C. J., Santos, S. R., Mahon, A. R., & Halanych, K. M. (2017). Geographic structure in the Southern Ocean circumpolar brittle star *Ophionotus victoriae* (Ophiuridae) revealed from mtDNA and single-nucleotide polymorphism data. *Ecology and Evolution*, *7*, 475–485. https://doi.org/10.1002/ece3.2617

Gargiulo, R., Kull, T., & Fay, M. F. (2020). Effective double-digest RAD sequencing and genotyping despite large genome size. *Molecular Ecology Resources*, *21*, 1037–1055. https://doi.org/10.1111/1755-0998.13314

Gilbert, K. J., Pouyet, F., Excoffier, L., & Peischl, S. (2020). Transition from background selection to associative Overdominance promotes diversity in regions of low recombination. *Current Biology*, *30*, 101–107.e3. https://doi.org/10.1016/j.cub.2019.11.063

Gillespie, J. M., & McClintock, J. B. (2007). Brooding in echinoderms: How can modern experimental techniques add to our historical perspective? *Journal of Experimental Marine Biology and Ecology*, *342*, 191–201. https://doi.org/10.1016/j.jembe.2006.10.055

González-Wevar, C. A., Hüne, M., Segovia, N. I., Nakano, T., Spencer, H. G., Chown, S. L., Saucède, T., Johnstone, G., Mansilla, A., & Poulin, E. (2017). Following the Antarctic circumpolar current: Patterns and processes in the biogeography of the limpet *Nacella* (Mollusca: Patellogastropoda) across the Southern Ocean. *Journal of Biogeography*, *44*, 861–874. https://doi.org/10.1111/jbi.12908

Grange, L. J., Peck, L. S., & Tyler, P. A. (2011). Reproductive ecology of the circumpolar Antarctic nemertean *Parborlasia corrugatus*: No evidence for inter-annual variation. *Journal of Experimental Marine Biology and Ecology*, *404*, 98–107. https://doi.org/10.1016/j.jembe.2011.04.011

Grange, L. J., Tyler, P. A., Peck, L. S., & Cornelius, N. (2004). Long-term interannual cycles of the gametogenic ecology of the Antarctic brittle star *Ophionotus victoriae*. *Marine Ecology Progress Series*, *278*, 141–155. https://doi.org/10.3354/meps278141

Griffiths, H., Van de Putte, A., & Danis, B. (2014). Data distribution: Patterns and implications. In C.De Broyer, P. Koubbi, H. Griffiths, B. Raymond, C. d'Udekem d'Acoz, A.Van de Putte, B. Danis, B. David, S. Grant, J. Gutt, C. Held, G. Hosie, F. Huettmann, A. Post, & Y. Ropert-Coudert (Eds.), *Biogeographic atlas of the Southern Ocean* (pp. 16–26). Scientific Committee on Antarctic Research.

Gutenkunst, R. N., Hernandez, R. D., Williamson, S. H., & Bustamante, C. D. (2009). Inferring the joint demographic history of multiple populations from multidimensional SNP frequency data. *PLoS Genetics*, *5*, e1000695. https://doi.org/10.1371/journal.pgen.1000695

Halanych, K. M., & Mahon, A. R. (2018). Challenging dogma concerning biogeographic patterns of Antarctica and the Southern Ocean. *Annual Review of Ecology, Evolution, and Systematics*, *49*, 355–378. https://doi.org/10.1146/annurev-ecolsys-121415-032139

Hemery, L. G., Eléaume, M., Roussel, V., Améziane, N., Gallut, C., Steinke, D., Cruaud, C., Couloux, A., & Wilson, N. G. (2012). Comprehensive sampling reveals circumpolarity and sympatry in seven mitochondrial lineages of the Southern Ocean crinoid species *Promachocrinus kerguelensis* (Echinodermata). *Molecular Ecology*, *21*, 2502–2518. https://doi.org/10.1111/j.1365-294X.2012.05512.x

Hodgson, D. A., Graham, A. G. C., Roberts, S. J., Bentley, M. J., Cofaigh, C. O., Verleyen, E., Vyverman, W., Jomelli, V., Favier, V., Brunstein, D., Verfaillie, D., Colhoun, E. A., Saunders, K. M., Selkirk, P. M., Mackintosh, A., Hedding, D. W., Nel, W., Hall, K., McGlone, M. S., … Smith, J. A. (2014). Terrestrial and submarine evidence for the extent and timing of the last glacial maximum and the onset of deglaciation on the maritime-Antarctic and sub-Antarctic islands. *Quaternary Science Reviews*, *100*, 137–158. https://doi.org/10.1016/j.quascirev.2013.12.001

Hoffman, J. I., Clarke, A., Linse, K., & Peck, L. S. (2011). Effects of brooding and broadcasting reproductive modes on the population genetic structure of two Antarctic gastropod molluscs. *Marine Biology*, *158*, 287–296. https://doi.org/10.1007/s0022 7-010-1558-6

Hohenlohe, P. A., Amish, S. J., Catchen, J. M., Allendorf, F. W., & Luikart, G. (2011). Next-generation RAD sequencing identifies thousands of SNPs for assessing hybridization between rainbow and westslope cutthroat trout. *Molecular Ecology Resources*, *11*, 117–122. https://doi.org/10.1111/j.1755-0998.2010.02967.x

Hugall, A. F., O'Hara, T. D., Hunjan, S., Nilsen, R., & Moussalli, A. (2016). An exon-capture system for the entire class Ophiuroidea. *Molecular Biology and Evolution*, 33, 281–294. https://doi.org/10.1093/molbev/msv216

Jacobs, S. S., Hellmer, H. H., & Jenkins, A. (1996). Antarctic ice sheet melting in the Southeast Pacific. *Geophysical Research Letters*, 23, 957–960. https://doi.org/10.1029/96GL00723

Janes, J. K., Miller, J. M., Dupuis, J. R., Malenfant, R. M., Gorrell, J. C., Cullingham, C. I., & Andrew, R. L. (2017). The $K = 2$ conundrum. *Molecular Ecology*, 26, 3594–3602. https://doi.org/10.1111/mec.14187

Jombart, T., & Ahmed, I. (2011). Adegenet 1.3-1: New tools for the analysis of genome-wide SNP data. *Bioinformatics*, 27, 3070–3071. https://doi.org/10.1093/bioinformatics/btr521

Jones, P., Binns, D., Chang, H. Y., Fraser, M., Li, W., McAnulla, C., McWilliam, H., Maslen, J., Mitchell, A., Nuka, G., Pesseat, S., Quinn, A. F., Sangrador-Vegas, A., Scheremetjew, M., Yong, S. Y., Lopez, R., & Hunter, S. (2014). InterProScan 5: Genome-scale protein function classification. *Bioinformatics*, 30, 1236–1240. https://doi.org/10.1093/bioinformatics/btu031

Jossart, Q., Sands, C. J., & Sewell, M. A. (2019). Dwarf brooder versus giant broadcaster: Combining genetic and reproductive data to unravel cryptic diversity in an Antarctic brittle star. *Heredity*, 123, 622–633. https://doi.org/10.1038/s41437-019-0228-9

Kamvar, Z. N., Tabima, J. F., & Grünwald, N. J. (2014). Poppr: An R package for genetic analysis of populations with clonal, partially clonal, and/or sexual reproduction. *Peer J*, 2, e281. https://doi.org/10.7717/peerj.281

Kelly, J. K., & Hughes, K. A. (2019). Pervasive linked selection and intermediate-frequency alleles are implicated in an evolve-and-resequencing experiment of *Drosophila simulans*. *Genetics*, 211, 943–961. https://doi.org/10.1534/genetics.118.301824

Korneliussen, T. S., Albrechtsen, A., & Nielsen, R. (2014). ANGSD: Analysis of next generation sequencing data. *BMC Bioinformatics*, 15, 356. https://doi.org/10.1186/s12859-014-0356-4

Kott, P. (1969). Zoogeographic discussion. In *Antarctic Ascidiacea* (pp. 193–208). American Geophysical Union (AGU). https://doi.org/10.1002/9781118668801.ch9

Lau, C. U., & Strugnell, J. M. (2022). Is the Southern Ocean ecosystem primed for change or at the cliff edge? *Global Change Biology*, 28, 4493–4494. https://doi.org/10.1111/gcb.16224

Lau, C. Y., Wilson, N. G., Silva, C. N. S., & Strugnell, J. M. (2020). Detecting glacial refugia in the Southern Ocean. *Ecography*, 43, 1639–1656. https://doi.org/10.1111/ecog.04951

Lau, S. C. Y., Strugnell, J. M., Sands, C. J., Silva, C. N. S., & Wilson, N. G. (2021). Evolutionary innovations in Antarctic brittle stars linked to glacial refugia. *Ecology and Evolution.*, 11, 17428–17446. https://doi.org/10.1002/ece3.8376

Lawrence, J. M., & Herrera, J. (2000). Stress and deviant reproduction in echinoderms. *Zoological Studies*, 39, 151–171.

Lesturgie, P., Planes, S., & Mona, S. (2021). Coalescence times, life history traits and conservation concerns: An example from four coastal shark species from the indo-Pacific. *Molecular Ecology Resources*, 22, 554–566. https://doi.org/10.1111/1755-0998.13487

Li, H., & Durbin, R. (2009). Fast and accurate short read alignment with burrows-wheeler transform. *Bioinformatics*, 25, 1754–1760. https://doi.org/10.1093/bioinformatics/btp324

Li, H., Handsaker, B., Wysoker, A., Fennell, T., Ruan, J., Homer, N., Marth, G., Abecasis, G., Durbin, R., & 1000 Genome Project Data Processing Subgroup. (2009). The sequence alignment/map format and SAMtools. *Bioinformatics*, 25, 2078–2079. https://doi.org/10.1093/bioinformatics/btp352

Linse, K., Cope, T., Lörz, A.-N., & Sands, C. (2007). Is the Scotia Sea a Centre of Antarctic marine diversification? Some evidence of cryptic speciation in the circum-Antarctic bivalve *Lissarca notorcadensis* (Arcoidea: Philobryidae). *Polar Biology*, 30, 1059–1068. https://doi.org/10.1007/s00300-007-0265-3

Liu, X., & Fu, Y. X. (2015). Exploring population size changes using SNP frequency spectra. *Nature Genetics*, 47, 555–559. https://doi.org/10.1038/ng.3254

Liu, X., & Fu, Y. X. (2020). Stairway plot 2: Demographic history inference with folded SNP frequency spectra. *Genome Biology*, 21, 280. https://doi.org/10.1186/s13059-020-02196-9

Locarnini, R. A., Mishonov, A. V., Baranova, O. K., Boyer, T. P., Zweng, M. M., Garcia, H. E., Reagan, J. R., Seidov, D., Weathers, K., Paver, C. R., & Smolyar, I. (2018). In A. Mishonov (Ed.), *World Ocean atlas 2018, Volume 1: Temperature*. NOAA Atlas NESDIS 81.

Love, A. C. (2003). Evolutionary morphology, innovation, and the synthesis of evolutionary and developmental biology. *Biology and Philosophy*, 18, 309–345. https://doi.org/10.1023/A:1023940220348

Marchi, N., & Excoffier, L. (2020). Gene flow as a simple cause for an excess of high-frequency-derived alleles. *Evolutionary Applications*, 13, 2254–2263. https://doi.org/10.1111/eva.12998

Matschiner, M., Hanel, R., & Salzburger, W. (2009). Gene flow by larval dispersal in the Antarctic notothenioid fish *Gobionotothen gibberifrons*. *Molecular Ecology*, 18, 2574–2587. https://doi.org/10.1111/j.1365-294X.2009.04220.x

Mazet, O., Rodríguez, W., Grusea, S., Boitard, S., & Chikhi, L. (2016). On the importance of being structured: instantaneous coalescence rates and human evolution—lessons for ancestral population size inference? *Heredity*, 116(4), 362–371. https://doi.org/10.1038/hdy.2015.104

McClintock, J. B. (1994). Trophic biology of Antarctic shallow-water echinoderms. *Marine Ecology Progress Series*, 111, 191–202.

McGee, M. D., Borstein, S. R., Neches, R. Y., Buescher, H. H., Seehausen, O., & Wainwright, P. C. (2015). A pharyngeal jaw evolutionary innovation facilitated extinction in Lake Victoria cichlids. *Science*, 350, 1077–1079. https://doi.org/10.1126/science.aab0800

Meirmans, P. G. (2020). GENODIVE version 3.0: Easy-to-use software for the analysis of genetic data of diploids and polyploids. *Molecular Ecology Resources*, 20, 1126–1131. https://doi.org/10.1111/1755-0998.13145

Moczek, A. P., Sultan, S., Foster, S., Ledón-Rettig, C., Dworkin, I., Nijhout, H. F., Abouheif, E., & Pfennig, D. W. (2011). The role of developmental plasticity in evolutionary innovation. *In Proceedings of the Royal Society B: Biological Sciences*, 278, 2705–2713. https://doi.org/10.1098/rspb.2011.0971

Moore, J. M., Carvajal, J. I., Rouse, G. W., & Wilson, N. G. (2018). The Antarctic circumpolar current isolates and connects: Structured circumpolarity in the sea star *Glabraster Antarctica*. *Ecology and Evolution*, 8, 10621–10633. https://doi.org/10.1002/ece3.4551

Moreau, C., Danis, B., Jossart, Q., Eléaume, M., Sands, C., Achaz, G., Agüera, A., & Saucède, T. (2019). Is reproductive strategy a key factor in understanding the evolutionary history of Southern Ocean Asteroidea (Echinodermata)? *Ecology and Evolution*, 9, 8465–8478. https://doi.org/10.1002/ece3.5280

Moreau, C., Saucède, T., Jossart, Q., Agüera, A., Brayard, A., & Danis, B. (2017). Reproductive strategy as a piece of the biogeographic puzzle: A case study using Antarctic Sea stars (Echinodermata, Asteroidea). *Journal of Biogeography*, 44, 848–860. https://doi.org/10.1111/jbi.12965

Muñoz-Ramírez, C. P., Barnes, D. K. A., Cárdenas, L., Meredith, M. P., Morley, S. A., Roman-Gonzalez, A., Sands, C. J., Scourse, J., & Brante, A. (2020). Gene flow in the Antarctic bivalve Aequiyoldia eightsii (jay, 1839) suggests a role for the Antarctic peninsula coastal current in larval dispersal: Gene flow patterns in *a. eightsii*. *Royal Society open. Science*, 7, 200603. https://doi.org/10.1098/rsos.200603

Nikula, R., Fraser, C. I., Spencer, H. G., & Waters, J. M. (2010). Circumpolar dispersal by rafting in two sub-Antarctic kelp-dwelling crustaceans. *Marine Ecology Progress Series*, 405, 221–230. https://doi.org/10.3354/meps08523

O'Hara, T. D., Hugall, A. F., Thuy, B., Stöhr, S., & Martynov, A. V. (2017). Restructuring higher taxonomy using broad-scale phylogenomics: The living Ophiuroidea. *Molecular Phylogenetics and Evolution*, 107, 415–430. https://doi.org/10.1016/j.ympev.2016.12.006

O'Hara, T. D., Hugall, A. F., Woolley, S. N. C., Bribiesca-Contreras, G., & Bax, N. J. (2019). Contrasting processes drive ophiuroid phylodiversity across shallow and deep seafloors. *Nature*, 565, 636–639. https://doi.org/10.1038/s41586-019-0886-z

Oksanen, J., Blanchet, F. G., Kindt, R., Legendre, P., Minchin, P. R., O'Hara, R. B., Simpson, G. L., Solymos, P., Stevens, M. H. H., & Wagner, H. (2013). *Vegan: Community ecology package. R Package Version 2.5–6*.

Pearse, J. S., Mooi, R., Lockhart, S. J., & Brandt, A. (2009). Brooding and species diversity in the Southern Ocean: Selection for brooders or speciation within brooding clades? In I. Krupnik, M. A. Lang, & S. E. Miller (Eds.), *Smithsonian at the poles: Contributions to international polar year science* (pp. 181–196). Smithsonian Institution Scholarly Press. https://doi.org/10.5479/si.097884601X.13

Pfeifer, B., Wittelsbürger, U., Ramos-Onsins, S. E., & Lercher, M. J. (2014). PopGenome: An efficient swiss army knife for population genomic analyses in R. *Molecular Biology and Evolution*, 31, 1929–1936. https://doi.org/10.1093/molbev/msu136

Phillips, M. J. (2009). Branch-length estimation bias misleads molecular dating for a vertebrate mitochondrial phylogeny. *Gene*, 441, 132–140. https://doi.org/10.1016/j.gene.2008.08.017

Pickrell, J. K., & Pritchard, J. K. (2012). Inference of population splits and mixtures from genome-wide allele frequency data. *PLoS Genetics*, 8, e1002967. https://doi.org/10.1371/journal.pgen.1002967

Pina-Martins, F., Silva, D. N., Fino, J., & Paulo, O. S. (2017). Structure_threader: An improved method for automation and parallelization of programs structure, fast Structure and MavericK on multicore CPU systems. *Molecular Ecology Resources*, 17, e268–e274. https://doi.org/10.1111/1755-0998.12702

Portik, D. M., Leaché, A. D., Rivera, D., Barej, M. F., Burger, M., Hirschfeld, M., Rödel, M. O., Blackburn, D. C., & Fujita, M. K. (2017). Evaluating mechanisms of diversification in a Guineo-Congolian tropical forest frog using demographic model selection. *Molecular Ecology*, 26, 5245–5263. https://doi.org/10.1111/mec.14266

Poulin, E. (2002). Evolutionary versus ecological success in Antarctic benthic invertebrates. *Trends in Ecology & Evolution*, 17(5), 218–222. https://doi.org/10.1016/s0169-5347(02)02493-x

Poulin, É., & Féral, J.-P. (1996). Why are there so many species of brooding antarctic echinoids? *Evolution*, 50, 820–830. https://doi.org/10.1111/j.1558-5646.1996.tb03891.x

Pritchard, J. K., Stephens, M., & Donnelly, P. (2000). Inference of population structure using multilocus genotype data. *Genetics*, 155, 945–959. https://doi.org/10.1093/genetics/155.2.945

Privé, F., Luu, K., Vilhjálmsson, B. J., & Blum, M. G. B. (2020). Performing highly efficient genome scans for local adaptation with R package pcadapt version 4. *Molecular Biology and Evolution*, 37, 2153–2154. https://doi.org/10.1093/molbev/msaa053

Puechmaille, S. J. (2016). The program structure does not reliably recover the correct population structure when sampling is uneven: Subsampling and new estimators alleviate the problem. *Molecular Ecology Resources*, 16, 608–627. https://doi.org/10.1111/1755-0998.12512

QGIS Development Team. (2019). *QGIS geographic information system. Open Source Geospatial Foundation Project*. http://qgis.osgeo.org/

Raupach, M. J., Thatje, S., Dambach, J., Rehm, P., Misof, B., & Leese, F. (2010). Genetic homogeneity and circum-Antarctic distribution of two benthic shrimp species of the Southern Ocean, *Chorismus antarcticus* and *Nematocarcinus lanceopes*. *Marine Biology*, 157, 1783–1797. https://doi.org/10.1007/s00227-010-1451-3

Revelle, W. (2020). Psych: Procedures for Personality and Psychological Research. https://CRAN.R-Project.Org/Package=psych

Riesgo, A., Taboada, S., & Avila, C. (2015). Evolutionary patterns in Antarctic marine invertebrates: An update on molecular studies. *Marine Genomics*, 23, 1–13. https://doi.org/10.1016/j.margen.2015.07.005

Roberts, R. E., Powell, D., Wang, T., Hall, M. H., Motti, C. A., & Cummins, S. F. (2018). Putative chemosensory receptors are differentially expressed in the sensory organs of male and female crown-of-thorns starfish, *Acanthaster planci*. *BMC Genomics*, 19, 853. https://doi.org/10.1186/s12864-018-5246-0

Sands, C. J., Griffiths, H. J., Downey, R. V., Barnes, D. K. A., Linse, K., & Martín-Ledo, R. (2013). Observations of the ophiuroids from the West Antarctic sector of the Southern Ocean. *Antarctic Science*, 25, 3–10. https://doi.org/10.1017/S0954102012000612

Sands, C. J., O'Hara, T. D., Barnes, D. K. A., & Martín-Ledo, R. (2015). Against the flow: Evidence of multiple recent invasions of warmer continental shelf waters by a Southern Ocean brittle star. *Frontiers in Ecology and Evolution*, 3, 63. https://doi.org/10.3389/fevo.2015.00063

Sands, C. J., O'Hara, T. D., & Martín-Ledo, R. (2021). Pragmatic Assignment of Species Groups Based on Primary Species Hypotheses: The Case of a Dominant Component of the Southern Ocean Benthic Fauna. *Frontiers in Marine Science*, 8. https://doi.org/10.3389/fmars.2021.723328

Simms, A. R., Milliken, K. T., Anderson, J. B., & Wellner, J. S. (2011). The marine record of deglaciation of the South Shetland Islands, Antarctica since the last glacial maximum. *Quaternary Science Reviews*, 30, 1583–1601. https://doi.org/10.1016/j.quascirev.2011.03.018

Sokolov, S., & Rintoul, S. R. (2009). Circumpolar structure and distribution of the Antarctic circumpolar current fronts: 1. Mean circumpolar paths. *Journal of Geophysical Research: Oceans*, 114, C11018. https://doi.org/10.1029/2008JC005108

Stöhr, S., O'Hara, T. D., & Thuy, B. (2012). Global diversity of brittle stars (Echinodermata: Ophiuroidea). *PLoS One*, 7, e31940. https://doi.org/10.1371/journal.pone.0031940

Strugnell, J. M., Allcock, A. L., & Watts, P. C. (2017). Closely related octopus species show different spatial genetic structures in response to the Antarctic seascape. *Ecology and Evolution*, 7, 8087–8099. https://doi.org/10.1002/ece3.3327

Thatje, S., Hillenbrand, C. D., & Larter, R. (2005). On the origin of Antarctic marine benthic community structure. *Trends in Ecology and Evolution*, 20, 534–540. https://doi.org/10.1016/j.tree.2005.07.010

Thom, G., Xue, A. T., Sawakuchi, A. O., Ribas, C. C., Hickerson, M. J., Aleixo, A., & Miyaki, C. (2020). Quaternary climate changes as speciation drivers in the Amazon floodplains. *Science Advances*, 6, aeax4718. https://doi.org/10.1126/sciadv.aax4718

Thompson, A. F., Stewart, A. L., Spence, P., & Heywood, K. J. (2018). The Antarctic slope current in a changing climate. *Reviews of Geophysics*, 56, 741–770. https://doi.org/10.1029/2018RG000624

Turner, R. L., & Dearborn, J. H. (1979). Organic and inorganic composition of post-metamorphic growth stages of *Ophionotus hexactis* (E.a. Smith) (Echinodermata: Ophiuroidea) during intraovarian incubation. *Journal of Experimental Marine Biology and Ecology*, 36, 41–51. https://doi.org/10.1016/0022-0981(79)90099-6

Verheye, M. L., Backeljau, T., & d'Udekem d'Acoz, C. (2016). Looking beneath the tip of the iceberg: Diversification of the genus Epimeria on the Antarctic shelf (Crustacea, Amphipoda). *Polar Biology*, 36, 925–945. https://doi.org/10.1007/s00300-016-1910-5

Wagner, A. (2011). The molecular origins of evolutionary innovations. *Trends in Genetics*, 27, 397–410. https://doi.org/10.1016/j.tig.2011.06.002

Wakita, D., Hayase, Y., & Aonuma, H. (2019). Different synchrony in rhythmic movement caused by morphological difference between five- and six-armed brittle stars. *Scientific Reports*, *9*, 8298. https://doi.org/10.1038/s41598-019-44808-w

Wakita, D., Kagaya, K., & Aonuma, H. (2020). A general model of locomotion of brittle stars with a variable number of arms. *Journal of the Royal Society Interface*, *17*, 20190374. https://doi.org/10.1098/rsif.2019.0374

Weber, A. A.-T., Abi-Rached, L., Bernard, G. A., Montoya-Burgos, I., & Chenuil, A. (2017). Positive selection on sperm ion channels in a brooding brittle star: Consequence of life-history traits evolution. *Molecular Ecology*, *26*, 3744–3759. https://doi.org/10.1111/mec.14024

Whitlock, M. C., & Lotterhos, K. E. (2015). Reliable detection of loci responsible for local adaptation: Inference of a null model through trimming the distribution of FST. *American Naturalist*, *186*, S24–S36. https://doi.org/10.1086/682949

Wilkie, I. C., Barbaglio, A., Maclaren, W. M., & Candia Carnevali, M. D. (2010). Physiological and immunocytochemical evidence that glutamatergic neurotransmission is involved in the activation of arm autotomy in the featherstar *Antedon mediterránea* (Echinodermata: Crinoidea). *Journal of Experimental Biology*, *213*, 2104–2115. https://doi.org/10.1242/jeb.039578

Wilson, N. G., Maschek, J. A., & Baker, B. J. (2013). A species flock driven by predation? Secondary metabolites support diversification of slugs in Antarctica. *PLoS One*, *8*, e80277. https://doi.org/10.1371/journal.pone.0080277

Wood, D. E., & Salzberg, S. L. (2014). Kraken: Ultrafast metagenomic sequence classification using exact alignments. *Genome Biology*, *15*, R46. https://doi.org/10.1186/gb-2014-15-3-r46

Wright, S. (1943). Isolation by distance. *Genetics*, *28*, 114–138. https://doi.org/10.1093/genetics/28.2.114

Xavier, J. C., Brandt, A., Ropert-Coudert, Y., Badhe, R., Gutt, J., Havermans, C., Jones, C., Costa, E. S., Lochte, K., Schloss, I. R., Kennicutt, M. C., & Sutherland, W. J. (2016). Future challenges in Southern Ocean ecology research. *Frontiers in Marine Science*, *3*, 94. https://doi.org/10.3389/fmars.2016.00094

Zweng, M. M., Reagan, J. R., Seidov, D., Boyer, T. P., Antonov, J. I., Locarnini, R. A., Garcia, H. E., Mishonov, A. V., Baranova, O. K., Weathers, K. W., Paver, C. R., & Smolyar, I. V. (2018). World Ocean atlas 2018, Volume 2: Salinity. In A. Mishonov (Ed.), *World Ocean atlas 2018*. NOAA Atlas NESDIS 82.

SUPPORTING INFORMATION

Additional supporting information can be found online in the Supporting Information section at the end of this article.